Talanta 238 (2022) 123048

Contents lists available at ScienceDirect

Talanta

journal homepage: www.elsevier.com/locate/talanta

Emerging trends in point-of-care sensors for illicit drugs analysis

Manisha Dagar [a], Sangeeta Yadav [b,c], V.V.R. Sai [a], Jitendra Satija [c], Himanshu Bhatia [d,*]

[a] Biomedical Engineering Laboratory, Department of Applied Mechanics, Indian Institute of Technology Madras, Chennai, 600036, India
[b] School of Bioscience and Technology, Vellore Institute of Technology, Vellore, Tamil Nadu, 632014, India
[c] Centre for Nanobiotechnology, Vellore Institute of Technology, Vellore, Tamil Nadu, 632014, India
[d] Ricovr Healthcare Inc, 252 Nassau St., Princeton, NJ, 08542, USA

ARTICLE INFO

Keywords:
Biosensor
Drug of abuse
Illicit drug
Optical sensors
Electrochemical sensor

ABSTRACT

Consumption of illicit narcotic drugs and fatal or criminal activities under their influence has become an utmost concern worldwide. These drugs influence an individual's feelings, perceptions, and emotions by altering the state of consciousness and thus can result in serious safety breaches at critical workplaces. Point-of-care drug-testing devices have become the need-of-the-hour for many sections such as the law enforcement agencies, the workplaces, etc. for safety and security. This review focuses on the recent progress on various electrochemical and optical nanosensors developed for the analysis of the most common illicit drugs (or their metabolites) such as tetrahydrocannabinol (THC), cocaine (COC), opioids (OPs), amphetamines & methamphetamine, and benzodiazepine (BZDs). The paper also highlights the sensitivity and selectivity of various sensing modalities along with evolving parameters such as real-time monitoring and measurement via a smart user interface. An overall outlook of recent technological advances in point of care (POC) devices and guided insights and directions for future research is presented.

1. Introduction

Drugs of abuse are legal and illegal substances that are typically consumed for their psychoactive effects and are often associated with dependence and addiction. These include substances like marijuana, tobacco, cocaine (COC), heroin, steroids, methamphetamine (M-AMP), as well as prescription drugs like opioids (OPs), dextromethorphan, and stimulants. Owing to their euphoric and sedating effects, these drugs impair thinking and judgment ability which may affect a person mentally as well as physically. This may be detrimental for situations that essentially require precise hand-eye coordination like driving, operating heavy machinery, or performing similar activities. In the past few decades, the prevalence of drug addiction has increased substantially worldwide which may be correlated with an increase in drug trafficking, a rise in the income of consumers, and poor implementation of government policies. According to World Drug Report 2020 released by United Nations Office on Drugs and Crime (UNODC), around 269 million people have used drugs in 2018, which corresponds to 5.4% global population aged 15–64 [1]. Amongst these, around 35.6 million people are estimated to suffer from drug-associated disorders which correspond to a global prevalence of drug-use disorders of 0.7% of the population aged 15–64.

Among the various classes of illicit drugs, cannabis (also known as marijuana) is predominantly consumed due to its easy availability, decriminalization, and legalization in some places in western countries for medical and recreational purposes [2]. According to the World Drug Report 2020, cannabis is the most used drug with an estimate of 3.9% of the global population (*viz.* about 192 million people) aged 15–64 [1]. Among adolescents and young adults, this drug has gained more popularity which is evident from the National Institute of Drug Abuse Report 2019, where annual marijuana prevalence levels were 11.8%, 28.8%, and 35.7% among the 8th, 10th, and 12th graders respectively [3]. After cannabis, OPs are of major concern due to their deleterious effects and health complications. In 2017, it accounted for 66% of the estimated 167,000 deaths associated with drug-use disorders [1]. In 2018, the number of deaths due to drug overdose has been recorded to be more than 67,000 in the US alone where OPs resulted in 70% of deaths along with fentanyl. The use of illicit drugs has not only affected the health of an individual, but it also has a very close liaison with the rapidly growing occurrence of crimes and socioeconomic issues [4]. A secondary analysis of a 2013 National Drug Strategy Household Survey report reveals a net loss of 3 billion in Australia alone due to absenteeism and

* Corresponding author.
E-mail address: himanshu.bhatia@ricovr.com (H. Bhatia).

https://doi.org/10.1016/j.talanta.2021.123048
Received 9 August 2021; Received in revised form 3 November 2021; Accepted 6 November 2021
Available online 8 November 2021

Table 1
Overview of cutoff concentration of different illicit drugs detection as per Substance Abuse and Mental Health Services Administration (SAMHSA [12]).

Illicit drug	Initial test cutoff concentration (immunoassay) (ng/mL)	Confirmatory test analyte (GC-MS)	Confirmatory test cutoff concentration (ng/mL)
Marijuana metabolites	50	THCA	15
Cocaine metabolites	150	Benzoylecgonine	100
Opiate metabolites	2000	Codeine	2000
Codeine/Morphine		Morphine	2000
6-Acetylmorphine	10	6-Acetylmorphine	10
Amphetamines	500	Amphetamine	250
AMP/MAMP		Methamphetamine	250
MDMA	500	MDMA	250
		MDA	250
		MDEA	250

Footnote: THCA = Δ^9-tetrahydrocannabinol-9-carboxylic acid; MDMA = Methylenedioxymethamphetamine; MDA = Methylenedioxyamphetamine; MDEA = Methylenedioxyethylamphetamine.

decreased output/performance leading to loss of profits for the companies [5].

As the crises of drug abuse continue to spread across the world, law enforcement is turning to a new generation of technology to expose drug trafficking, smugglers, and to identify victims of drug abuse. In this regard, the point of care (POC) diagnostic devices that can offer rapid, sensitive, specific, and on-site identification of drugs may play a vital role in controlling drug abuse. Such devices will ease the screening of the employees (pre-employment and during employment), legal professionals (to screen for driving under the influence), and medical professionals (for addiction and rehab centers). To provide an extremely valuable output, results demonstrated by these drug detection tools need to be more informative and should reveal the presence or absence of the consumed illicit drug substance quantitatively. This along with minimizing illicit drug abuse may improve workplace productivity and their socio-economic balance.

Current illicit drug detection techniques are based on qualitative and quantitative analysis of biological specimens such as urine, blood, saliva, hair, breath, and sweat. Although these methods are conducive in some cases, these have several methodological limitations [6–8]. Drug detection still relies on conventional systems like the use of specific sophisticated instruments such as mass spectrometer, gas chromatography, high-performance liquid chromatography, and ELISA kit. Most of these techniques ensure good sensitivity and specificity, however, these suffer from several disadvantages like tedious pretreatment of samples, the requirement of trained professionals, high cost of assay, and prolonged assay time [9–11]. To cite an example, the detection kits from Neogen Corporation cost more than 230 dollars per plate are extremely expensive and take more than an hour to detect methadone in the sample. Furthermore, the requirement of biological samples like blood or urine for drug detection makes it inconvenient for field applications such as places of high risk like roadside traffic stops. Hence, there is a pressing need for a robust sensor that can surpass the existing limitations and meet the ever-growing demand and thus help in maintaining the public safety, health, and socio-economic balance. In the case of decentralized detection of drug abuse, the sensors ideally should be hand-held, easily implemented, and suitable for high-throughput screening with high specificity and sensitivity.

Recent technological advancements in material science and bioanalytical methods and their convergence with nanoscience and nanotechnology have led to the development of numerous ultra-sensitive sensors for illicit drug detection. This review presents a detailed overview of the current state of the art of the sensors developed for the detection of the five most commonly used illicit drugs, i.e. cannabis, COC, OPs, AMPs & their substitutes, and benzodiazepines (BZDs). The sensor matrix composition, mechanism of sensing, and various performance parameters of these electrochemical and optical sensors are discussed in detail. Further, the potential strategies to be adopted for the successful translation and commercialization of these technologies are highlighted as prospects.

Table 2
Overview of electrochemical and optical sensor technologies developed for THC detection.

Transducing mechanism	Sensor matrix	Sample matrix	LOD	Sensor characteristics	References
Chronoamperometry	SPCE	Saliva	79.6 nM	DR = 79.6–159 nM Analysis time = 30 s	[24]
SWV	SPCE/AuNPs	PBS Urine	22.29 pM (PBS)	DR = 31.84 pM-31.84 μM (PBS) Analysis time = 20–40 min RP = 88–115% (urine)	[26]
DPV	MIP-CNT in micropipette tubes	KCl (1:1 methanol-water)	0.57 nM	DR = 3.84–796 nM	[27]
Amperometry	GCE-AuNPs-thionine -chitosan-HRP	PBS Serum	10.5 pM	DR = 0.03–3184 nM Analysis time = 10 min RP = 98.2–101.5% (serum)	[28]
CV	GCE	Methanol	1.082 nM	DR = 7.64–35.98 nM Analysis time = 30 s	[29]
Amperometry	MWCNT/SPCE	Saliva	0.5 μM	Analysis time = 6 min	[30]
Impedance spectroscopy	Gold electrode/PET substrates	Saliva	308 pM	DR = 0.318–318 nM Analysis time = 60 s	[31]
FAIMS	FAIMS microchip	Methanol	0.207 μM	DR = 0.207–1.274 μM	[32]
Chemiresistor	s-SWCNTs/IDE	Breath	0.163 ng (vapor phase detection)	Analysis time = few seconds	[33]
Fluorescence	PE-fluorescent particles	Saliva	0.03 nM	DR = 0.03–318 nM	[34]
TLC-SERS	Diatomaceous earth-AuNPs	Urine	31.85 μM	DR = 31.85–3185 μM	[35]

Footnotes: CV = Cyclic voltammetry; CNT = Carbon nanotube; DPV = Differential pulse voltammetry; DR = Dynamic range; FAIMS = Field asymmetric ion mobility spectrometry; GCE = Glassy carbon electrode; AuNPs = Gold nanoparticles; HRP = Horseradish peroxidase; IDE = Interdigitated gold electrodes; LOD = limit of detection; MIP = Molecular imprinted polymers; MWCNT = Multi-walled carbon nanotubes; PBS = Phosphate buffer saline; PE = Phycoerythrin; PET = Polyethylene terephthalate substrates; RP = Recovery percentage; SWV = Square wave voltammetry; SERS = Surface-enhanced Raman spectroscopy; SPCE = Screen-printed carbon electrode; s-SWCNTs = semiconductor-enriched single-walled carbon nanotube; TLC = Thin-layer chromatography.

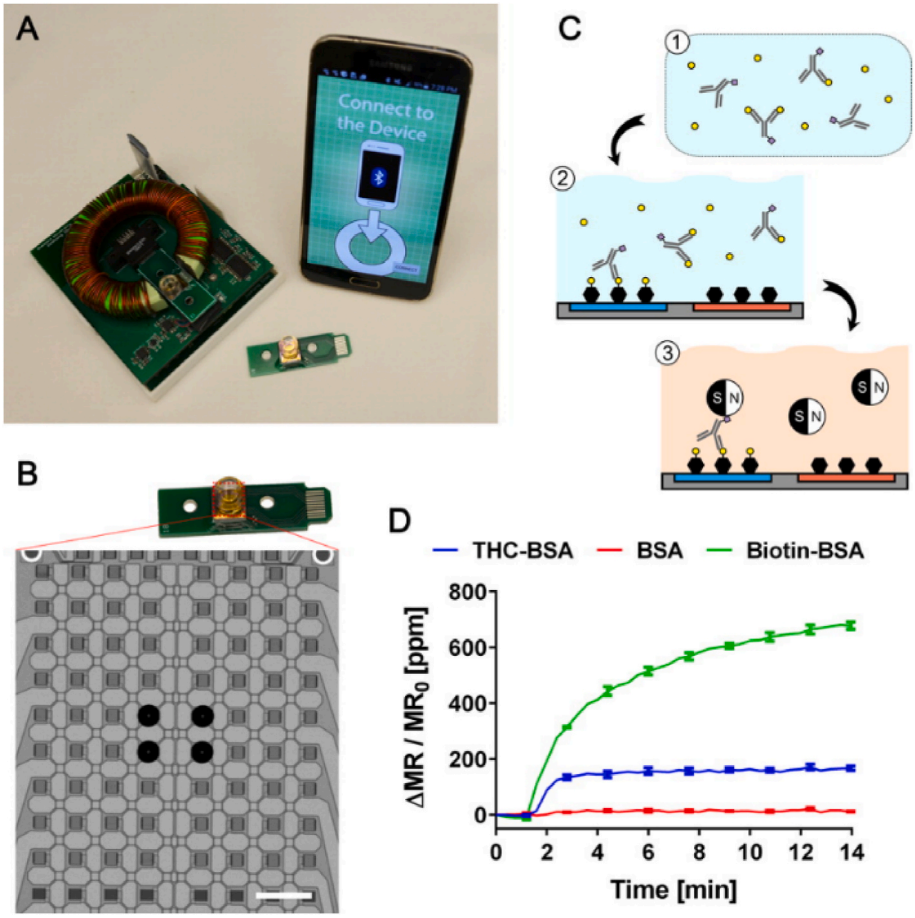

Fig. 1. GMR biosensor platform for detection of THC by following the competitive assay; (A) Left: a measurement reader consisting of a toroid core coil, electrical circuits, and bluetooth module. Middle: a disposable cartridge is based on a customized design of printed circuit board (PCB) integrated with a GMR biosensor chip and reaction well. Right: a smartphone with a customized app, (B) Disposable cartridge showing the GMR biosensor chip wire-bonded to the customized PCB and the reaction well glued on top of the chip, (C) Schematic illustration of the competitive assay, and (D) Real-time signal recording. Reprinted with permission from Ref. [36]. Copyright (2016) American Chemical Society.

2. Sensors for illicit drug analysis

Overconsumption of drugs causes severe health implications and the level of the risk varies with the individual and the type of drug used. Therefore, the detection of these drugs at their cutoff level with high selectivity and sensitivity is the need of the hour (Table 1). This section gives an account of (i) the characteristics of various drugs with the main focus on tetrahydrocannabinol (THC), COC, OPs, AMPs & M-AMPs, and BZDs, and (ii) the technological advancements to realize the electrochemical and optical sensors along with their analytical performance attributes.

2.1. Sensors for tetrahydrocannabinol

Cannabis is a psychoactive drug that is derived from plant species *Cannabis sativa, Cannabis indica,* and *Cannabis ruderalis* [13]. THC is one of the main psychoactive constituents of cannabis, but cannabidiol, cannabinol, tetrahydrocannabivarin, cannabigerol, cannabichromene, and hundreds of other cannabinoids also show dose-dependent psychoactive effects such as euphoria, anxiety, enhancement of sensory perception, tachycardia, antinociception, impaired psychomotor performance, cognitive function paranoia, pseudohallucinations, and depersonalization [14,15]. Although FDA has approved synthetic THC and several other cannabis-derived drugs for medical use under the supervision of the medical practitioner, the sale of the products containing these drugs is tightly regulated. To monitor and control the illegal supply and usage of these drugs, sensing devices play an important role by preferentially detecting these drugs in the environment or biological samples.

Intensive research has been carried out to develop POC devices for THC detection, while a few are available commercially such as OraLine®, Cozart® RapiScan, Oratect® II, OraLab®6, Toxiquick®, OrAlert®, Rapid STAT®, and DrugWipe® 5/5+. Many of these technologies suffer from specificity as these give a positive response in the presence OPs, M-AMP, COC, and AMP. In addition, many of these devices do not meet the Roadside Testing Assessment (ROSITA), ROSITA-2, and Driving under the Influence of Drugs (DRUID) standards, as the sensitivities of these devices are 75% or less, which is below the minimum recommended value of 80% [16,17]. Another drawback of these technologies is the use of lateral flow assays (LFA) kits which generate large variations in the sensor response particularly in the variable field conditions [18]. Additionally, several other factors like variation in standardized test concentration (1–30 ng/mL), prolonged response time (2–30 min), cold-weather constraints, no specific sample volumes, and low THC concentration due to dry mouth are important reasons that are responsible for their limited applications and hence have paved the way for the search of a novel, field deployable robust sensor [19,20].

Progress in the field of sensors and assays for THC detection has helped to address a few of these challenges and to realize some ultrasensitive detection techniques (Table 2). Particularly, the development of assays for quantifying metabolites of cannabis such as Δ^9-THC, THC-COOH, 11-OH-THC has gained more popularity [21–23]. For example, a screen-printed carbon electrode (SPCE) functionalized with *N*-(4-amino-3-methoxyphenyl)-methanesulfonamide mediator has been developed for Δ^9-THC sensing in saliva [24]. In the presence of Δ^9-THC, the mediator is galvanostatically oxidized to give an electrochemically active adduct which could be detected by chronoamperometric reduction. The sensor could detect 25–50 ng/mL of Δ^9-THC in the saliva in a short duration of 30 s. The developed sensor showed sensitivity, specificity, and accuracy of 28%, 99%, and 52%, respectively when employed

for the real sample sensing from cannabis smokers. Although the sensor demonstrated ultrafast detection of Δ^9-THC in unmodified saliva, the sensitivity of the device was lower than acceptable and hence requires further modifications to meet the desired standards for forensic practices [25].

The convergence of nanotechnology with polymer chemistry and their integration with sensor technologies has been leveraged with several innovative analytical methods and devices. In this line of research, considerable effort has been made to develop an ultrasensitive electrochemical sensor for Δ^9–THC detection by imbibing carbon nanotube (CNT) and molecularly imprinted polymers (MIPs) in the sensor matrix [27]. Here, the CNT offers high electrical conductivity, porosity, and large surface area whereas MIPs are being used as receptors for their high specificity, inherent stability, low cost, and ease of synthesis. The hydrophobic interaction of Δ^9-THC with MIP (synthesized by copolymerization of methacrylic acid (MAA) and ethylene glycol dimethacrylate (EDGMA)) facilitates its selective binding and subsequently, it gets oxidized and results in a prominent differential pulse voltammetry (DPV) signal with a limit of detection (LOD) of 0.18 ng/mL. Besides the high sensitivity and selectivity, the MIP-based sensor demonstrated superior reusability and robustness and thus proved its potential as a futuristic POC diagnostic device.

Very often cannabis is consumed with alcohol leading to a synergistic phenomenon with more adverse effects and in such cases, road-side rapid detection of both THC and alcohol is quite challenging. To tackle this issue, Mishra et al. have reported a novel wearable dual-analyte sensor ring system with a combination of two electrochemical techniques, i.e. voltammetry and amperometry [30]. In this sensor system, the ring cover was designed with multi-walled carbon nanotubes (MWCNTs)-coated carbon electrode for selective THC detection, while a Prussian-blue transducer functionalized with alcohol oxidase/chitosan reagent layer was employed for the biosensing of alcohol. The potentiostat circuit embedded within the ring body facilitated the on-spot selective detection of alcohol, whereas THC could be detected with a defined square wave voltammetry (SWV) peak at +0.3 V with no false alarms. This dual sensor demonstrated the LOD of 0.5 μM in the diluted saliva sample within 3 min, which was capable of detecting THC even after 24 h of cannabis consumption. This wearable sensing system has immense potential to be utilized for the rapid roadside testing of various other illicit drugs also by simply substituting the chemical or biochemical reaction.

In a different approach, Lee et al. developed a unique sensing platform by integrating the giant magnetoresistive (GMR) biosensor with a portable reader system and smartphone to detect THC in saliva by employing a competitive assay (Fig. 1) [36]. This small biosensor has a disposable chip cartridge with 80 sensors that can be independently functionalized for multiplexed assays. Moreover, this chip has an inbuilt feature of a bluetooth connection that enables POC quantification and compatibility with laptop and smartphone. Further, this device has the unique advantage of a toroidal core coil which can apply an external magnetic field at low power consumption owing to its compact circuit board design and easy portability. The mechanism of THC sensing relies upon a competitive assay in the two reaction wells, where the control well is immobilized with bovine serum albumin (BSA), and the reaction well is coated with THC conjugated BSA (THC-BSA). Initially, the sample of interest is pre-incubated with biotinylated antibodies against THC for 15 min, which is followed by the addition of this mixture in both wells. This allows the binding of unoccupied antibodies with THC-BSA followed by washing and introduction of streptavidin-coated magnetic nanoparticles (MNPs), and then signal measurement. The bounded MNPs disturb the stray field of magnetization of the biosensor and thus alter the resistance, which is monitored as GMR signals ($\Delta MR/MR_0$). The changes in the GMR signal were observed to be directly proportional to the number of bound MNPs which was inversely proportional to THC concentration in the sample due to the competitive nature of the assay. Under optimized conditions, with a simple saliva collection technique, the portable sensor could measure THC in the range from 0 to 50 ng/mL with the detection limit of 5 ng/mL. Rapid and precise detection of THC in saliva along with the technical feasibility for on-site screening advocate the implementation of GMR biosensor in POC settings. Further, this technology could be explored in near future to establish the cutoff concentration of other illicit drugs or for multiplexed measurement.

In yet another example, an affinity-based smart electrochemical biosensor was realized for detection of THC in saliva [31]. The sensor was based on non-faradaic electrochemical impedance spectroscopy (EIS) that measured the alteration in the dielectric properties at the electrode-electrolyte interface upon binding of THC-BSA to anti-THC antibody. This sensor could successfully predict the varying concentrations of THC in saliva by applying different learning algorithms via regression analysis, providing a high performance of area under the receiver operating characteristic curve (0.951) with high specificity and sensitivity within 1 min of assay time. Under optimized conditions, the sensor demonstrated 100 pg/mL detection limit and 100 pg/mL-100 ng/mL dynamic range (DR). This device exhibited promising results with additional advantages like portability, low battery-power requirement, and disposable saliva swap embedded in sensors that make it suitable for on-site detection.

Plouffe et al. developed two different LFA-based on POC testing devices where gold nanoparticles (AuNPs) (size = 6 nm) and phycoerythrin fluorescent particles (size = 50 nm) were used for colorimetric and fluorimetry based detection of THC [34]. In the presence of THC, a sandwich immunocomplex of capture antibody, THC, and detector antibody-NP conjugate was formed, which could be visualized through photographs or naked eye in the colorimetric mode. In the fluorescent mode, a charged-coupled device (CCD) camera with the appropriate optical filter was employed to measure the signal intensity. The AuNPs based assay could detect THC level up to 5 ng/mL, whereas the fluorescent particles-based assay achieved the LOD of 0.01 ng/mL, which indicates better sensitivity of the fluorescent-based assay. To illustrate field deployment, validation of the LFA kit is essentially required and further to realize into POC device, integration of this kit with portable fluorescence reader is strongly required which will make this device robust with further improvement in the sensitivity.

The surface-enhanced Raman scattering (SERS) technique has also been investigated for THC detection due to its inherent high sensitivity and selectivity [37,38]. Particularly, hybrids of photonic crystal-plasmonic SERS substrates, fabricated with diatom photonic crystals on which AuNPs were deposited, have been shown to detect THC levels down to 10 ppb [39]. However, the requirement of a confocal Raman microscope is one of the important limiting factors for the field application of this technology. To address this issue, the use of a portable Raman spectrometer with an efficient thin-layer chromatography (TLC) based SERS substrate has been proposed by Sivashanmugan et al. [35]. In this strategy, diatomaceous earth particles were used as a stationary phase with two-dimensional (2D) periodic pores inherently possessing large surface area, high porosity, high adsorption capacity, and ample hydroxyl groups at the bio-silica surface [40,41]. During the field trial, drop-casting of a urine sample was followed by elution using chloroform-acetone-ammonium hydroxide (40/20/40 *v/v*) mixture (i.e. mobile phase) which developed a separate THC spot. Subsequently, a colloidal solution of AuNPs (~60 nm) was added to the spot and the Raman signal was measured by a portable Raman spectrometer which depicted the characteristic peak for THC at 1603 cm^{-1}. Although this procedure is highly sensitive and selective with a portable Raman instrument, the tedious procedure of TLC-based separation is not suited for on-site detection.

Recently, Brunelle et al. developed a noninvasive strategy to detect THC metabolite from the sweat present on the fingerprints [42]. This strategy involved the sample collection on polyethylene film followed by micro-centrifugation in methanol and incubation in the microtiter well with the conjugate of THC and horseradish peroxidase (HRP) enzyme, leading to a competitive immunoassay between THC-HRP and THC

Table 3
Overview of electrochemical and optical sensor technologies developed for cocaine detection.

Transducing mechanism	Sensor matrix	Sample matrix	LOD	Sensor characteristics	References
Amperometry	pAb–COC–MBs-CH8 sensor array	PBS Urine Saliva Serum	0.29 nM (PBS/Saliva) 1.18 nM (urine) 2.07 nM (serum)	RP = 112.7–116.7% (urine) RP = 89.4–115.8% (saliva) RP = 88.0–110.7% (serum)	[54]
DPV	CdTe QDs-GCE	PBS Serum	5.0 pM	DR = 50–450 pM Analysis time = 45 min RP = 96.15–98.25% (serum)	[55]
DPV	GO/AuNPs/SPCE	PBS	1 nM	DR = 1–500 nM	[56]
DPV	AuNPs/GCE	PBS Serum	0.5 pM	DR = 5 pM - 5 nM Analysis time = 45 min RP = 98–103.5% (serum)	[57]
Amperometry	Cytochrome P450 2B4/SPCE	PBS	0.2 mM	DR = 0.2–1.2 mM	[58]
CV	Ab-MBs/SPE	Water Saliva Urine	0.47 pM (water)	Analysis time = 25 min RP = 88–106% (saliva) RP = 89–94% (urine)	[59]
EIS	NanoMIPs/GSPE	Water	0.70 nM	DR = 0.30–147 nM	[60]
Chemiluminescence	MB/AuNRs/HRP	PBS	0.48 nM	DR = 1–10 nM Analysis time = 6 min	[61]
Fluorescence	MIP/Mn-doped-ZnS QDs	Saliva Serum	115 nM (saliva) 49.5 nM (serum)	RP = 98–104% (saliva)	[62]
Fluorescence	GO/ICSDA	Water Urine Mixed drug samples	190 nM (water)	DR = 0.2–100 μM (water) DR = 0.5–100 μM (urine) RP = 93.2–100.6% (phenacetin) RP = 86.7–108.0% (diltiazem) RP = 82.2–97.0% (levamisole)	[63]
Colorimetry	AuNP-L-cyst/ZnSeS QDs	Water	128 nM	DR = 20–100 μM	[64]
EWF	Aptamer/FSP-AAP-Optical fiber	PBS	10.5 μM	DR = 10–5000 μM Analysis time = 16.5 min	[65]

Footnotes: AAP = amino-modified anchor DNA probe; AuNPs = Gold nanoparticles; AuNRs = Gold nanorods; CdTe = Cadmium telluride; CV = Cyclic voltammetry; DPV = Differential pulse voltammetry; DR = Dynamic range; EIS = Electrochemical impedance spectroscopy; EWF = Evanescent wave fibre; FSP = Fluorescence-labeled short DNA probe; GCE = Glassy carbon electrode; GO = Graphene oxide; GSPE = Gold screen-printed electrode; HRP = Horseradish peroxidase; ICSDA = Isothermal circular strand-displacement amplification; LOD = Limit of detection; MIP = Molecular imprinted polymer; pAb–COC–MBs = Anti-cocaine antibodies on protein G functionalized magnetic microbeads; PBS = Phosphate buffer saline; QDs = Quantum dots; RP = Recovery percentage; SPCE = Screen-printed carbon electrode; SPE = Screen-printed electrode.

metabolites for their binding towards the capture anti-THC antibodies on the sensor surface. The THC metabolite and the enzyme-tagged conjugate compete with each other as the antigens for the system. Thereafter, a solution of 2,2′-azino-bis(3-ethylbenzothiazoline-6-sulphonic acid) (ABTS, enzyme-substrate), H_2O_2, and citrate buffer were added into the well, which reacted with the HRP turning the solution into blue-green color following which the intensity of the solution was measured by spectroscopy. Since the antibody utilized in this assay had a greater affinity towards the metabolite, absorbance was found to be decreased with an increased concentration of metabolite due to the lesser binding of the enzyme-tagged conjugate. Overall, this system could quantify cannabis uses in a Yes/No format with a sensitivity range of 5.0 nM–100 nM. The low detection capabilities, ability to discriminate between a narrow concentration range with the simple and flexible nature of the competitive immunoassay combined with an optical readout establish this technique to be immediately translated in a lateral flow assay kit/strip as it would require little or no scientific training.

At present, the detection of illicit drugs through potential breath analysis platforms has also gained attention, where devices for THC detection have made promising advancements [43–45]. These platforms utilize techniques such as field asymmetric ion mobility spectrometry (FAIMS) that principally ionizes the molecules by charge transfer followed by their separation based on mobility in microchip channel with varying dispersion field (DF, 0–60 kV cm^{-1}) in a compensation voltage of −6 and +6 V for these ions to reach the detector [32]. While both cations and anions move in the channel, they could be detected simultaneously by a charge collector generating spectra in both polarities. This method has been used for THC detection at a specific compensation voltage of 0.72 V under DF of 55%, which could achieve the LOD value of 65 ppm. Recently developed semiconductor-enriched single-walled carbon nanotube (s-SWCNTs) chemiresistors based prototype could detect the ultra-low levels (down to 0.163 ng) of THC in different samples using machine learning (ML) classifiers [33]. However, such systems require a significant amount of preliminary testing and standardization to be applied for law enforcement applications. Liquid chromatography-tandem mass spectrometry (LC-MS/MS) based breath samples analysis has also shown the highly accurate quantitative determination of THC and demonstrated the LOD of 5 pg/pad (present in Exabreath® device used to trap the drug from aerosol breath) in the breath sample collected over a 2 min period [46,47]. Despite its high sensitivity, there is a lack of ease of sample handling and portability along with the price and thus limiting their on-site applications.

2.2. Sensors for cocaine

COC is a white crystalline alkaloid derived from the leaves of *Erythroxylon coca* (generally known as coca plant) and is widely used as a local anesthetic due to its vasoconstrictor properties. COC is a highly addictive drug due to its stimulant and euphoric properties that directly affect the nervous system including the brain. Within minutes of abuse through intravenous injection or inhalation, it enters systemic circulation resulting in relief from fatigue and euphoria, enhancement in the mental alertness and thereby energizing the user. It is slowly absorbed from the nasal and gastrointestinal tract with a peak plasma concentration of 200–600 ng/mL within 30–120 min, and as a result, several thousands of ng/min can be measured in intoxicated individuals [48]. Prolonged use of COC causes addiction, paranoia, anxiety disorders, sleep problems, mental confusion, convulsions, and ultimately death [49]. Owing to its potential side effects, on-spot detection and quantification of COC are required which is possible by developing simple, easy, sensitive, and accurate strategies through many technological hybrids.

To date, numerous sensing modalities have been implemented to

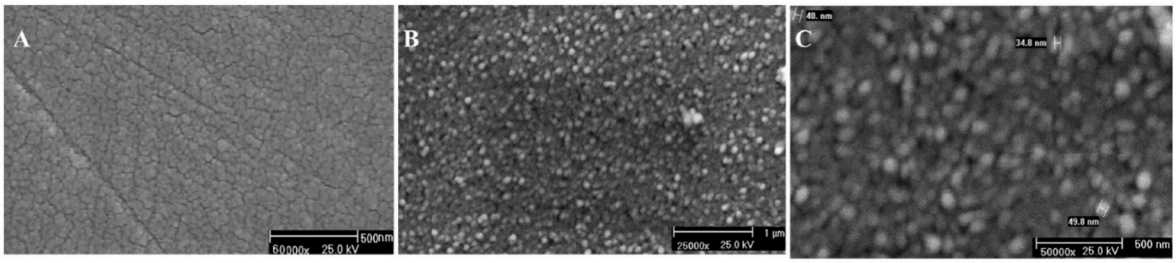

Fig. 2. SEM image of (A) the bare GCE, (B and (C) the AuNPs deposited GCE at two different magnification levels. Reprinted from Ref. [57], Copyright (2016), with permission from Elsevier.

detect COC (Table 3). Notably, electrochemical methodologies are mainly based on direct, receptor-based, immunoassay, and nanopore-based sensing. In the direct methods, the enzymatic or non-enzymatic reaction of COC is observed at the electrodes like SPCE [50,51] or glassy carbon electrode (GCE) modified with functional nanomaterial [52]. For example, SPCE functionalized with the mixture of cytochrome P450 2B4 enzyme and carbon ink has been utilized for sensitive detection of COC [53]. This sensor relies on the enzymatic reaction leading to *N*-demethylation of the tertiary amine in the COC to produce norcocaine that gives an amperometric sensitive response. Under optimized conditions, an excellent LOD of 23 nM could be achieved with good repeatability (RSD = 3.56%). Such direct electrochemical methods are very simple since analytical signals are directly proportional to COC concentration with the desired selectivity even at the nanomolar level of detection limit. However, testing in the biological samples like urine, saliva, and blood using the direct method is not suitable due to oxidation of interfering agents along with the COC which might result in false positive signal.

In an interesting approach, Bauer et al. combined a noncompetitive immunoenzymometric assay with online detection of the alkaline phosphatase (ALP) enzyme-labeled antibody to develop an amperometric biosensor for indirect detection of COC [66]. In this method, the analyte cocaine is first interacted with an enzyme-labeled polyclonal anti-cocaine antibody forming a COC-pAb-ALP complex. This was followed by the separation of the unbound labeled antibodies using an affinity column containing a perfusion chromatography carrier modified by immobilized cocaine. The free pAb-ALP was retained in the column while the COC-pAb-ALP could be collected in the column effluent and quantified by ALP enzyme-mediated hydrolysis of phenyl phosphate to phenol. Although this method is quite tedious, it could detect COC down to 380 pM level. Although this automated amplified flow immunoassay technique has several advantages, low recovery (49 ± 3%) indicates the pressing need for additional investigation and optimization to realize this into a POC device. On the other hand, a hybrid microfluidic electrochemical ELISA device containing monoclonal antibodies grafted magnetic nano-beads and HRP showed the detection limit down to 0.15 ng/L [59]. Though these antibodies or enzymes based techniques are capable of detecting picomolar to nanomolar levels of the COC, these have several constraints that can affect the device performance such as pH variation, enzyme denaturation, and loss of functionality of biomolecules. Furthermore, inefficacy in the conformity of multi-component systems functioning and detection time are other common limitations of these techniques.

Aptamers are synthetic nucleic acids that have selective ligand binding properties with many inherent benefits such as inexpensive synthesis, small size, good stability, flexible design, and easy chemical modification [67,68]. To date, aptamers have been widely used as recognition elements for biosensor fabrication, especially for the detection of proteins and small molecule targets, and have been established as promising alternatives to antibodies. The aptamer-based sensors have been made more sensitive by integrating with nanomaterials like CNTs and their composites [69,70], quantum dots (QDs) [55], and graphene [56]. Roushani et al. developed a GCE/AuNPs-cystamine/HS-aptamer-AuNPs matrix-based electrochemical sensor platform that could achieve the LOD value of 0.5 pM for COC [57]. The presence of uniformly distributed AuNPs both on the surface of the GCE and at the end of the aptamer was ascribed for increased active surface area and faster electron transfer and thereby amplifying the electrochemical signal (Fig. 2).

In an advanced approach, nanopore technology, wherein the change in ionic current is measured in real-time across the pore due to the presence of the analyte, has been integrated with an aptamer-based sensor for COC detection. Kawano et al. developed an α-hemolysin based nanopore sensor through which a COC-selective DNA aptamer can pass through in the unbound state (Fig. 3) [71]. However, upon interaction with COC, the aptamer conformation changes and cannot pass through the pore and consequently blocks the pore which eventually generates large current differences. This sensor could generate the

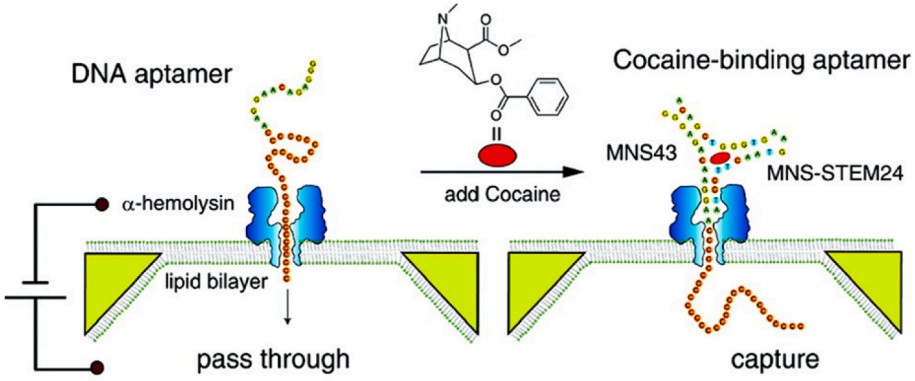

Fig. 3. Schematic presentation of cocaine sensing using α-hemolysin biological nanopore and the cocaine-binding aptamer. The DNA aptamer can pass through the pore in the absence of cocaine (left), whereas the presence of cocaine changes its conformation and block the pore, and doesn't allow it to pass through the channel (right). Reprinted with permission from Ref. [71]. Copyright (2011) American Chemical Society.

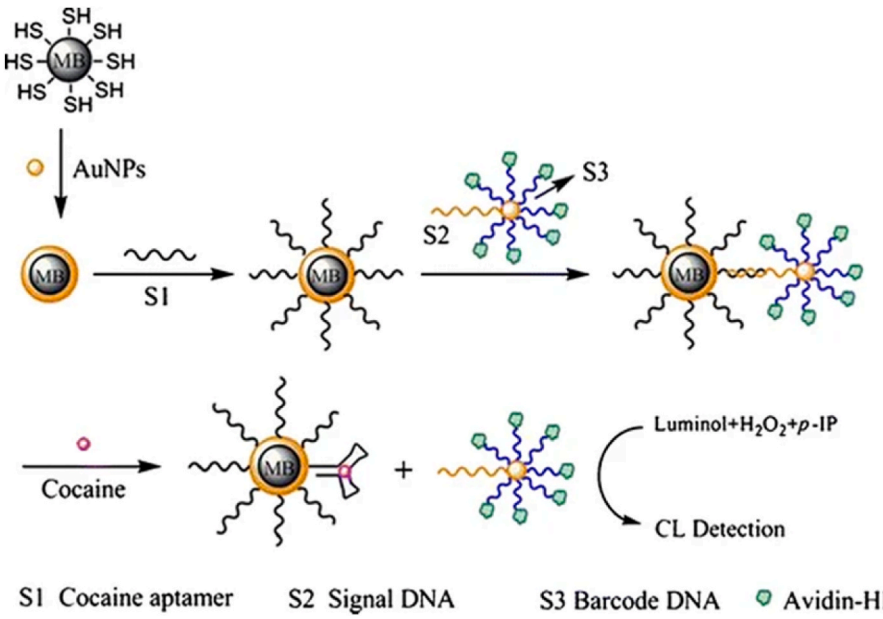

Fig. 4. Schematic (a) illustration for the chemiluminescence-based sensing of COC using gold nanoprobes and functionalized magnetic microbeads. Reprinted by permission from Springer Nature: Springer, Analytical and Bioanalytical Chemistry [61], Copyright (2011). (For interpretation of the references to color in this figure legend, the reader is referred to the Web version of this article.)

Table 4
Overview of electrochemical and optical sensor technologies developed for the detection of opioids.

Opioids	Transducing mechanism	Sensor matrix	Sample matrix	LOD	Sensor characteristics	References
Morphine	DPV	SPE	Urine	5.2 nM	DR = 0.017–7.01 μM	[82]
	DPV	GNSs/GCE	PBS	0.4 μM	DR = 1–65 μM	[83]
	DPV	dsDNA/MBA/Au electrode	PBS Plasma Urine	0.01 μM (PBS)	DR = 0.05–500 μM (PBS) RP = 97–104.9% (plasma) RP = 103.2–105.8% (urine)	[84]
	Amperometry	Pt–Co NAE	PBS Serum	7.83 μM (PBS)	DR = 23.5 μM - 2.39 mM (PBS) RP = 99.6–108% (serum)	[85]
	SWV	MWCNTs/MIP/AuNPs/PGE	PBS Urine	2.9 nM (PBS)	DR = 0.008–5 μM (PBS) RP = 96.0–104.5% (urine)	[86]
	DPV	RhNPs/MC/GCE	PBS Serum	40 nM (PBS)	DR = 0.1–20 μM (PBS) RP = 95–108.5% (serum)	[87]
	UV–Vis spectrophotometery	MA-AuNPs	PBS Serum Urine	17 nM (PBS)	DR = 0.07–3 μM (PBS) RP = 94.6–107.1% (serum) RP = 98.3–107.7% (urine)	[88]
	Fluorescence immunoassay	FITC-labeled anti-MOR monoclonal antibody	PBS Urine	3.51 nM (PBS)	DR = 0.70–8.77 μM RP = 99.88–109.79% (urine)	[89]
	SWV	Gr/$CoFe_2O_4$/CPE	BRB Urine Plasma	0.011 μM (BRB)	DR = 0.03–12.0 μM (BRB) RP = 98.1–101.5% (urine) RP = 97.5–102% (plasma)	[90]
Codeine	DPV	$CoFe_2O_4$ NPs/CPE	Plasma Urine	20 nM	DR = 0.06–38 μM RP = 98–103% (urine) RP = 98–102% (plasma) Analysis time = 90 s	[91]
	DPV	Fe_3O_4-AuNPs/CNTs/GCE	PBS Serum	3.2 pM (PBS)	DR = 0.01–1 nM (PBS) DR = 10–900 nM (PBS)	[92]
	SPR	EGDMA/MAA/MIP membrane	Acetonitrile	10 fM	DR = 1 fM - 10 nM	[93]
	CSWV	SPCE	PBS	5 μM	DR = 5–100 μM	[94]
Fentanyl	DPV	SWCNT	PBS	11 nM	DR = 0.01–1 μM	[95]
	SWV	MWCNT/SPCE	PBS	10 μM	DR = 10–100 μM	[96]
	DPV	GCE/CNOs	PBS Serum Urine Ampoule	0.3 μM (PBS)	DR = 1–60 μM (PBS) RP = 98–103% (serum) RP = 96.60–104.70% (urine) RP = 103.4–105.5% (ampoule)	[97]

Footnotes: AuNPs = Gold nanoparticles; BRB = Britton-Robinson buffer; CNO = carbon nanoonions; CNT = Carbon nanotube; $CoFe_2O_4$ NPs = Cobalt ferrite nanoparticle; CPE = carbon paste electrode; CSWV = Cyclic square wave voltammetry; DPV = Differential pulse voltammetry; DR = Dynamic range; ds-DNA = Double-stranded DNA; EGDMA = Ethylene glycol dimethyl acrylic ester; FITC = Fluorescein isothiocyanate; GCE = Glassy carbon electrode; GNSs = Graphene nanosheets; Gr = Graphene; LOD = Limit of detection; MAA = Methacrylic acid; MA-AuNPs = Melamine modified gold nanoparticles; MBA = Mercapto-benzaldehyde; MIP = Molecular imprinted polymers; MOR = Morphine; MWCNT = Multi-walled carbon nanotubes; PBS = Phosphate buffer saline; PGE = Pencil graphite electrode; Pt–Co NAE = Pt–Co alloy nanowire array-modified electrode; RhNPs = Rhodium nanoparticles; RP = Recovery percentage; SPCE = Screen-printed carbon electrode; SPE = Screen-printed electrode; SWCNT = Single-walled carbon nanotubes; SWV = Square wave voltammetry.

response in 60 s at 300 ng/mL to 5 s at 30 μg/mL. In another approach, Wang et al. reported the COC sensing with an artificial nanopore, developed by etching the polyethylene terephthalate thin sheet, with a wide linear range of 1 nM–10 μM and LOD value of 1 nM [72]. The high electroanalytical output of miniaturized sensors (by making use of nano- or micro-electrodes and nanogap sensors), improved LOD, low-cost, high selectivity are some of the promising features of the electrochemical biosensors for their potential commercialization. Further improvisation requires statistical validation and successful translation for selective detection in real samples.

Similar to electrochemical techniques, efforts have been made to develop optical sensors also towards the detection of COC. For instance, SERS based aptameric sensor has been developed by using AgNPs film-coated polished gold disc as substrate wherein the binding of COC induces the transition in the aptamer molecule conformation resulting in an increase in the SERS signal intensity as a function of drug concentration [73]. This reagent-free aptamer sensor could detect 1 μM of COC with high selectivity. Li et al. proposed chemiluminescence (CL) biosensor using a bio-barcode assay in which COC-specific aptamers were immobilized on the AuNPs-functionalized magnetic microbeads (MB-AuNPs) and subsequently hybridized with the double functionalized gold nanoprobe (DF-AuNPs) consisting of aptamer-specific signal DNA and HRP to form MB-AuNPs/aptamer/DF-AuNPs (Fig. 4) [61]. When interacted with a sample containing COC, the aptamer changes its structure resulting in the dissociation of gold nanoprobe from the complex of MB-AuNPs/aptamer/DF-AuNPs, which was used for measurement of CL by means of HRP enzyme-mediated oxidation of luminol. A significant amplification could be achieved for the detection of COC by employing AuNPs as a multi-DNA-HRP carrier. This method exhibited good linearity in the range of 1–10 nM with a LOD value of 0.48 nM, even in presence of other interfering drug molecules such as caffeine and heroin. In another approach, the localized surface plasmon resonance (LSPR) property of AuNPs has been utilized to visually detect the COC in the concentration range of 20 nM–200 μM in 10 min [74]. In a different approach, Li et al. proposed a dark field microscopy (DFM) imaging-based nanoplasmonic strategy for identifying COC on the latent fingerprint [75]. The sensing was based on the cocaine-induced aggregation of the aptamer-functionalized AuNP to generate the LSPR signal by means of DFM which could detect in the range of 150 ng to 30 μg. Although this technique is very easy for on-site application, the risk of the false-positive signal is more due to environmental factors mediated aggregation of AuNPs such as various pH and temperature.

2.3. Sensors for opioids

OPs are alkaloids that are naturally derived from the plant *Papaver somniferum* and are mainly used as analgesic agents. These are classified as naturally occurring (e.g. codeine and morphine), semisynthetic derivatives (e.g. hydrocodone, hydromorphone, buprenorphine, and oxycodone), and synthetic derivatives (e.g. anilidopiperidine and diphenylpropylamine) [76]. These drugs bind to opioid receptors (ORs) which are widely distributed in the brain and the peripheral nervous system and activate them to trigger a biological response [77]. These receptors are prominent targets not only for painkillers but also for antidepressants, anti-addiction medications, and anti-anxiety drugs.

2.3.1. Sensors for morphine

Morphine is the most commonly prescribed medicine for its analgesic properties with a standard dose of 0.1–0.2 mg/kg and attains its peak plasma level within 15–20 min of intramuscular or subcutaneous administration, and within 30–90 min after oral administration [78,79]. However, morphine is addictive and prone to abuse and thereby influences various immune functions as well as disruption of the central nervous system, respiratory rate, and blood pressure [80]. Hence, strict monitoring of morphine in biological and environmental samples is essentially required. Traditionally, morphine detection in biological samples is carried out with the LC-MS/MS technique which displays good sensitivity in the range of 0.018–0.18 μM with LOD value of 2.10 μM [81]. However, time-consuming analysis, the requirement of large fluid samples & toxic solvents, and lack of field deployment are the major issues that have paved the way for the development of various alternate techniques by utilizing nanomaterials and other biochemical reactions (Table 4).

Morphine is electroactive in nature due to the presence of a phenolic ring and tertiary amine group that is catalyzed through an oxidative mechanism to form either pseudomorphine or normorphine depending upon the release of proton and electron [80]. This electroactive property of morphine has been utilized to develop a variety of electrochemical biosensors. A DPV based sensor developed using screen-printed electrode (SPE) depicted a dynamic range of 5 nM - 2 μM and LOD of 5 nM in the urine sample [82], while a graphene nanosheet/GCE based sensor matrix showed a dynamic range of 0.01–720 μM and LOD of 0.4 μM [83]. Similarly, a ds-DNA modified gold electrode demonstrated the linear detection range of 0.05–500 μM and LOD value of 0.01 μM both in human serum and urine samples [84], whereas an amperometric sensor employing Pt–Co alloy nanowire array in the matrix exhibited the dynamic range of 23–230 μM with the detection limit of 7.8 μM in human serum samples [85]. In another strategy, SWV sensor fabricated with AuNPs/MIP/MWCNT/pencil graphite electrode could achieve the LOD value of 90 nM (DR = 0.1–100 μM) in saliva [98] and 2.9 nM (DR = 0.08–5 μM) in human serum/urine samples [86]. The high sensitivity towards morphine detection in the biological fluids with good reliability and without the aid of any sample pre-treatment has proved the potential of this technology for its translation.

Optical detection of morphine by surface-plasmon-resonance (SPR) has also been realized in a competitive immunoassay format by employing the anti-morphine monoclonal antibody and morphine-bovine serum albumin (MO-BSA) conjugate (as a competitor) [99]. The MO-BSA immobilized gold chip showed a reduction in the SPR incident angle shift with an increase in the MO level due to its inhibition effect. The developed SPR sensor chip could achieve the linear detection range of 0.1–10 ng/mL. In a different study, Mohseni and Bahram (2016) proposed a simple colorimetric assay for naked-eye detection of morphine and codeine by employing melamine-modified AuNPs [88]. This method could selectively detect the analyte even in the presence of the biological interferents such as amino acids, and other drugs like tramadol, AMP, and M-AMP with LOD value of 17 nM (DR = 0.07–3 μM) for morphine and 9 nM (DR = 0.03–0.8 μM) for codeine in pharmaceuticals, urine, and blood serum samples. Furthermore, the developed method showed a good recovery rate in the range of 94.6–107.7% in the spiked injection, tablet, serum, and urine samples, establishing its commercial relevance. In another approach, Farahani et al. reported the application of L- and D-cysteine CdSe quantum dot (CdSe-QDs) towards highly selective detection of the L-morphine [100]. It was observed that the fluorescence intensities of L- and D-cysteine functionalized CdSe-QDs were quenched after interaction with L-morphine. The interaction between L-morphine and D-cysteine functionalized CdSe-QDs was observed to be more efficient and exhibited a detection limit of 0.06 μM. The sensor response, i.e. the extent of fluorescence quenching, was found to be L-morphine concentration-dependent according to the Stern-Volmer equation. This simple, inexpensive, quick, and sensitive fluorescence quenching-based optical sensor has the potential to realize into a POC device with a hand-held portable fluorescent reader.

In a recent study, chromium metal-organic framework nanoparticles [Cr(III)-MOF-NPs] have been exploited for rapid and highly sensitive, and selective detection of morphine [101]. The sensing mechanism was based on the hydrogen bond formation and host-guest interaction between electronegative morphine and Cr(III)-MOF-NPs, which causes a photoinduced transfer of electrons within the Cr(III)-MOF-NP structure and results in a blue shift in the characteristic emission band of the Cr (III)-MOF-NPs (from 593 to 566 nm) even in the presence of many competing matrices. Besides this, a prominent enhancement in

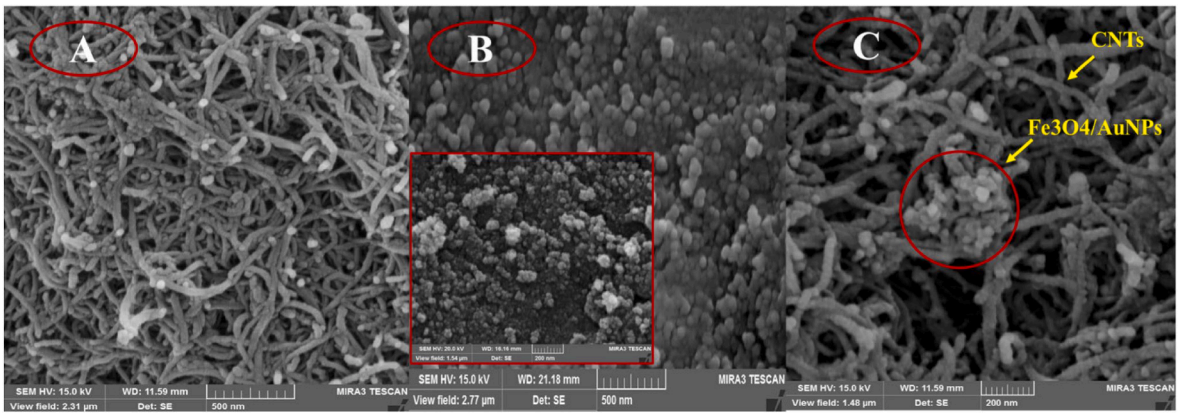

Fig. 5. Scanning electron microscopic image of CNTs/GC (A) Fe_3O_4/GC (B) and Fe_3O_4/AuNPs/CNTs/GC (C) modified electrodes showing the uniform distribution of the net-like spread of CNT and uniform distribution nanoparticles on the electrode surface. Reprinted by permission from Springer Nature: Journal of Materials Science: Materials in Electronics [92], Copyright (2019).

photoluminescence intensity and a visual color change from brown to yellow could also be observed with an increase in the concentration of morphine. Under the optimal experimental conditions, the optical chemosensor exhibited a stable response for morphine detection in a concentration range of 0.1–350 nM with detection and quantification limits of 0.167 and 0.443 nM, respectively. The capability of this chemosensor to quantify the morphine in the spiked serum and urine sample with a good recovery percentage proved its potential as future POC technology. In a different approach, a competitive fluorescence immunoassay, wherein morphine molecules competitively bind with FITC-labeled morphine antibody against hapten, achieved the detection limit of 3.5 nM with 99.8–109.7% recovery rate, implying its high potential for field application [89]. This simple, rapid, and sample-free pretreatment process can be easily integrated into a microarray platform to realize fluorescence-based microarray diagnostics which can be quite useful for mass screening.

2.3.2. Sensors for codeine

Codeine is used for its compelling analgesic properties as it causes less euphoria and sedation in comparison to morphine, but it is often abused by improper consumption. The quantification of codeine is usually hindered by its structural analog with several biological compounds leading to false positive or negative signals which are subdued by LC-MS/MS within a dynamic range of 0.017–0.17 μM and LOD of 0.67 nM in body fluids and tissue samples [81]. However, this technique requires a sophisticated lab set-up, expensive solvents, and trained professionals to carry out detection.

Square wave voltammetry-based electrochemical sensor developed by employing graphene-$CoFe_2O_4$ nanocomposite modified carbon paste electrode (CPE) attained the sensitive detection range of 0.03–12 μM with LOD of 0.025 μM for codeine when tested in human urine and serum samples [90]. The developed sensor provides a better alternative to conventional tools as it displays easy sample preparation and high selectivity towards codeine testing even in presence of interferents. Mashhadizadeh et al. utilized TiO_2 nanoparticles modified CPE to realize a DPV based electrochemical sensor for codeine detection [102]. The developed sensing approach could detect codeine with a detection limit of 0.018 μM with high sensitivity (0.409 $\mu A/\mu molL^{-1}$) and a wide linear range (0.07–100 μM). The usability of the voltammetric sensor could be successfully established for codeine determination in human plasma serum samples. In another example, a label-free electrochemical sensor derived with GCE functionalized with Fe_3O_4, AuNPs, and CNTs significantly improved the sensitivity as the presence of nanocomposite served as a signal amplifier by means of improving the immobilization efficiency of the aptamer probe and electron-transfer between the electrode and the $[Fe(CN)_6]^{3-/4-}$ redox probe [92]. The net-like homogeneous coating of CNTs with nanowire shape spread and uniformly distributed Fe_3O_4/AuNPs at the surface of the electrode offered a greater accessible surface area (Fig. 5). With this unique combination of properties of nanomaterials, the aptameric sensor could significantly achieve the LOD of 3.2 pM with two different linear detection ranges (0.01–1 nM and 10–900 nM). Further, the developed method could be successfully tested for codeine determination in the spiked human serum samples with a recovery rate of 96.2–103%.

A colorimetric assay utilizing the LSPR property of citrate-capped AuNPs has been developed for the quantification of codeine sulfate [103]. This assay was based on the ligand exchange reaction which involves the coordination complex formation between codeine molecules and AuNPs by replacing the citrate capping resulting in the aggregation of the nanoparticles and a prominent color change from red to blue. Under optimized conditions, this strategy showed a linear range from 1 to 10 μM with LOD of 0.9 μM even in the presence of morphine, phenylephrine, phenobarbital, diazepam, lorazepam, and clonazepam. The simplicity, economic viability, portability, and the capability of on-spot detection of suspected drugs are advantageous features of this technology, however, the highly sensitive nature of the AuNPs and tendency to form aggregates due to a minor change in pH or temperature might generate false-positive results and thus limits its applications. Zeng et al. proposed a molecularly imprinted polymer (methacrylic acid as monomer and ethylene glycol dimethyl acrylic ester as cross-linker) functionalized SPR chip for codeine detection [93]. This chip could detect codeine selectively in the mixed codeine-morphine acetonitrile solution with a lower limit of 10 fM indicating its potential towards a precise and sensitive detection of ultra-low levels of codeine.

2.3.3. Sensors for fentanyl

Fentanyl and its analogs are more potent drugs than morphine (e.g. carfentanil is 10,000 times more potent than morphine) and overdose of these drugs might cause serious clinical complications resulting in blue lips, breathing difficulty, foaming in the mouth, rigid body, and chest wall rigidity leading to death [104]. Fentanyl is a very short-acting drug and thus quickly becomes addictive to users for recreation. At present, the market landscape of commercial diagnostics has a limited FDA approval for onsite devices/kits for fentanyl or its analogs detection with exception of products based on ELISA for fentanyl, butyryl fentanyl, para-fluorobutyryl with 100% accuracy, while DRI (Thermo), Carolina Liquid Chemistries, and ARK Diagnostics do not have FDA approval along with cross-reactivity issues with fentanyl analogs [105–107].

Several research groups have demonstrated the proof of concepts for detecting fentanyl at micro-molar levels using electrochemical sensors. For instance, Barfidokht et al. developed the PalmSens technology that is a hand-held potentiostat sensor possessing flexible SPCE modified with a

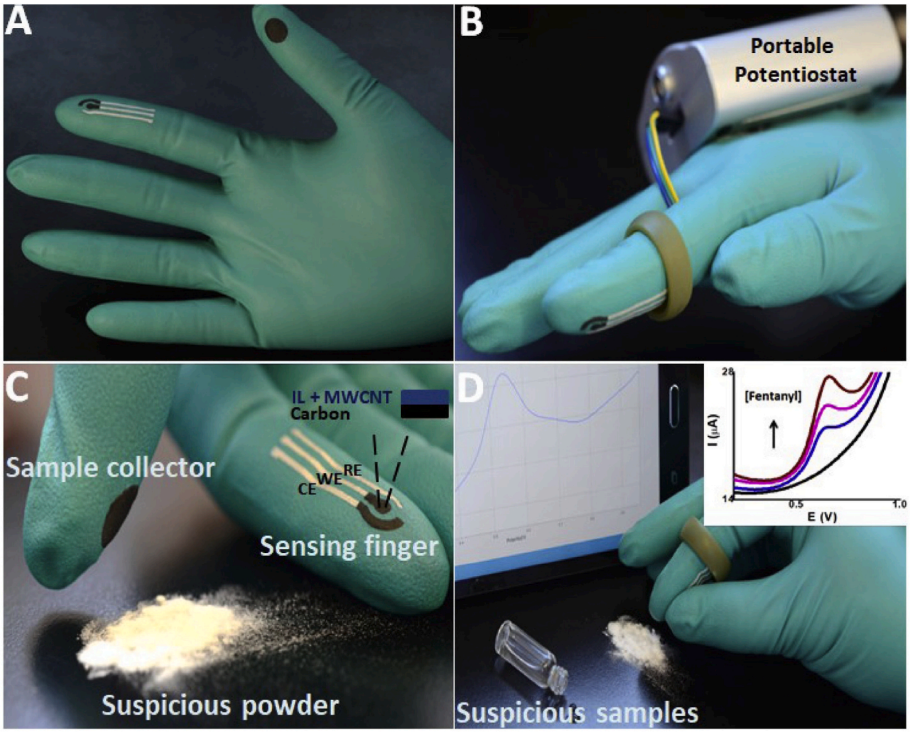

Fig. 6. Overview of Lab-on-a-Glove concept (swipe, scan, and sense) for on-site detection of fentanyl; (A) Photograph of glove containing sensing finger modified with ionic liquid/MWCNT composition and sample collector. (B) Image showing the glove-based sensor with a portable electroanalyzer (back-view). The electrodes are connected via wires and a modified ring to a PalmSens potentiostat for on-site detection with wireless communication to a smartphone for rapid analysis and reporting of the SWV results. (C) Image showing suspicious sample collection in the powder phase. (D) Joining of thumb (collector) and sensing (index) fingers after swiping a powder sample; inset shows the voltammograms of direct fentanyl detection in powder/liquid samples. Reprinted from Ref. [96], Copyright (2019), with permission from Elsevier.

mixture of MWCNTs and ionic liquid (4-(3-butyl-1-imidazolio)-1-butanesulfonate) (Fig. 6) [96]. This technology is based on a 'Lab-on-a-glove' concept and utilizes the thumb for collecting the sample, while the index finger, having MWCNTs/SPCE electrode is used for measuring the sensor response on a smartphone/tablet sent via a wrist-worn potentiostat. Upon voltammetric measurement, a linear sensor response could be obtained in the range of 10–100 μM concentration of fentanyl with a LOD value of 10 μM. This glove-based "swipe, scan, sense, and alert" strategy is very simple in use where the chemical analytics are brought to the user's fingers, which has opened up new possibilities for identifying drugs of abuse in an emergency. Sohouli et al. proposed another novel electrochemical sensing approach by employing carbon nano-onions (CNOs) in the sensor matrix due to their metal-like conductive behavior and excellent electrocatalytic activity [97]. The

Table 5
Overview of electrochemical and optical sensor technologies developed for detection of methamphetamines.

Transducing mechanism	Sensor matrix	Sample matrix	LOD	Sensor characteristics	References
SWSV EIS	SPE/MWCNTs-Nf/AuNPs	NaOH	6 nM (SWSV) 0.3 nM (EIS)	DR = 0.02–0.1 μM; (SWSV) DR = 1.15–26.9 nM (EIS)	[113]
SWV	CeO_2NP/rGO/GCE	BRB Plasma	8.7 μM	DR = 25–166.6 μM RP = 89.8–102.3%	[114]
SWV	GCE/MWCNT/AuNPs/Fe_3O_4@SiO_2	BRB Urine	16 nM	DR = 50 nM - 50 μM RP = 101–111%	[115]
SPR	MAMP-BSA/gold SPR chip	PBS Saliva	2.50 nM (PBS)	DR = 0.33–37.3 nM (PBS) Analysis time = 3 min RP = 113.2% (saliva)	[116]
SPR	AuNPs-BSA-Anti-MAMP	PBS Urine	1.1 nM (PBS)	DR = 6.7 nM - 6.7 μM RP = 83% Analysis time = 15 min	[117]
FFT-SWV	MIP/MWCNTs/CPE	NaOH Urine Serum	83 nM (NaOH)	DR = 10 nM - 100 μM (NaOH) RP = 94–104% (urine and serum)	[118]
Fluorescence	GQDs-MIP	PBS	0.011 μM	DR = 5–50 μM	[119]
Fluorescence	SiO_2/CQDs/ms-MIPs	PBS Plasma Urine	1.6 μM	DR = 5.0–250 μM RP = 99–105% (plasma) RP = 92–110% (urine)	[120]
SERS	AuNPs/SiO_2 microsphere	Saliva Urine	1 nM	DR = 5 nM - 10 μM (saliva) DR = 10 nM - 10 μM (urine)	[121]
SERS	MAMP aptamer-AuNPs	Serum	7 pM	DR = 10 pM to 10 nM RP = 94.3–107% (serum)	[122]

Footnotes = AuNPs = Gold nanoparticles; BRB = Britton-Robinson buffer; CeO_2NP = Cerium oxide nanoparticles; CPE = Carbon-paste electrode; CQDs = Carbon quantum dots; DR = Dynamic range; EIS = electrochemical impedance spectroscopy; FFT-SWV = Fast Fourier transform-square wave voltammetry; GQDs = graphene quantum dots; LOD = Limit of detection; MAMP-BSA = Methamphetamine-bovine serum albumin; MIPs = Molecularly imprinted polymers; ms = Mesoporous structure; MWCNT = Multiwalled carbon nanotube; Nf = Nafion; PBS = Phosphate buffer saline; rGO = Reduced graphene oxide; RP = Recovery percentage; SERS = Surface-enhanced Raman spectroscopy; SPR = Surface plasmon resonance; SPE = Screen-printed electrode; SWSV = Square wave stripping voltammetry; SWV = Square wave voltammetry.

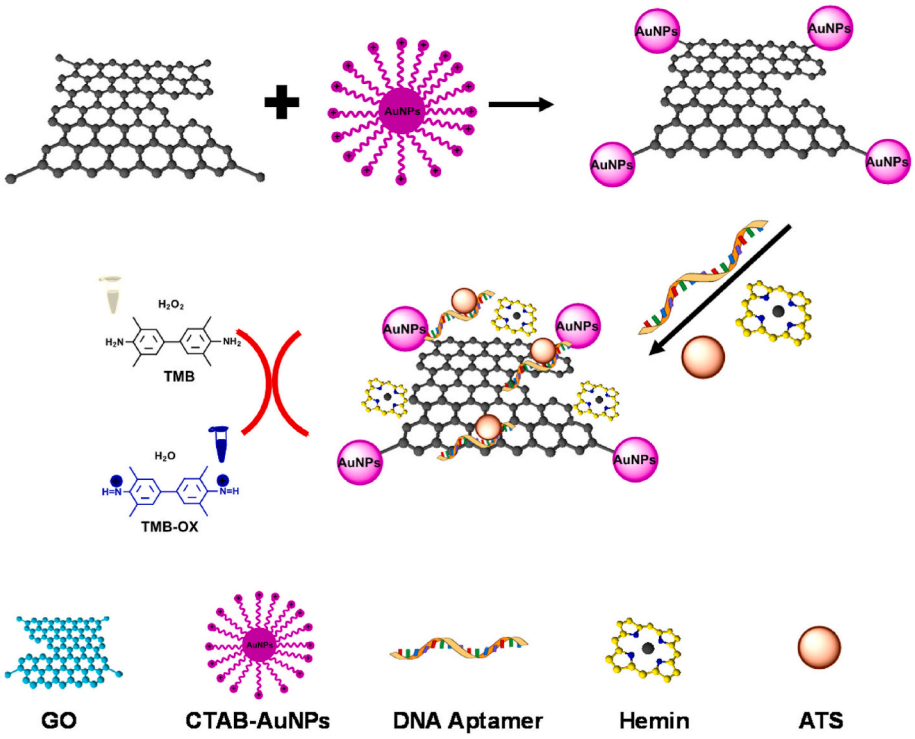

Fig. 7. (A) Schematic representation of the hybrid nanozyme peroxidase mimic aptamer-based biosensor for amphetamine-type stimulants (ATS) detection. GO is first bound to CTAB-AuNPs via electrostatic interaction to form a GO-AuNPs hybrid nanozyme complex. Thereafter, the DNA aptamer is bound to the GO-AuNPs hybrid nanozyme and captures the target ATS. Hemin is added to the system to enhance the catalytic signal followed by the catalytic oxidation of TMB by H_2O_2, generating a blue color complex specific to the target ATS concentration. Reprinted from Ref. [112], Copyright (2020), with permission from Elsevier. (For interpretation of the references to color in this figure legend, the reader is referred to the Web version of this article.)

sensor was developed by immobilizing the CNOs on a GCE which could detect the fentanyl linearly in the range of 1–60 μM with a detection limit of 0.3 μM in blood serum, urine, and ampoule. Given the importance of fentanyl analogs, limited research has been conducted on detection systems strategy for these analogs and therefore requires immediate attention by researchers.

2.4. Sensors for amphetamine and substituted amphetamines

This class of psychostimulant drugs acts by triggering the release of neurotransmitter dopamine through the dopamine-active transporter system leading to a sudden increase in energy, mood, auditory or visual perception [108]. Increased use of these drugs has raised the necessity for the fast screening of these drugs in the biological samples under the clinical settings and on-fields. The cut-off value for Europe and the USA are 500 and 1000 ng/mL, respectively, however, these biological levels of AMPs and substituted AMPs might have serious health implications [109]. For a long time, the color spot test based POC devices, e.g. Oral-Eze®, Draeger DrugTest®, RapidStat®, DrugWipe-5+, and OrAlert® are being used for the detection of AMPs [110,111]. Although these tests are convenient for on-site screening, the use of toxic corrosive substances and false-negative/-positive results associated with poor sensitivity are a few limitations.

Recent progress in the field of sensors has advocated the development of improved devices and strategies which offer highly sensitive and selective detection of the drugs in a short duration (Table 5). For example, Adegoke et al. reported a hybrid nanozyme based optical detection technique for rapid aptameric biosensing of AMP-type stimulants [112]. In this approach, a hybrid nanozyme complex was judiciously designed by electrostatically immobilizing the graphene oxide (GO) to cetyltrimethylammonium bromide (CTAB)-capped AuNPs possessing DNA aptamer (receptive for AMPs stimulants like AMP, M-AMP, MDMA) (Fig. 7). The interaction of the drug with this nanozyme complex induces the amplification of catalytic signals by hemin and oxidation of 3,3,5,5-tetramethylbenzidine (TMB) by peroxidase to generate a blue color of varying intensity as a function of AMPs concentration. The K_{cat} value for M-AMP was observed to be 3-fold higher than AMPs in the presence of TMB suggesting an increased level of oxidized substrate generation per nanozyme per second relative to AMP. The LOD values were observed to be 154 nM (28.6 ng/mL) and 185 nM (34.1 ng/mL) for

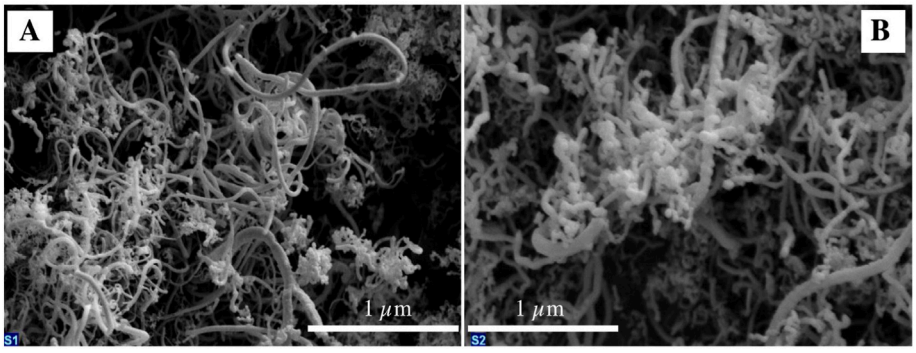

Fig. 8. (A) SEM images of the SPE surface modified with MWCNTs-Nf and (B) MWCNTs-Nf/AuNPs. Reprinted from Ref. [113], Copyright (2015), with permission from Elsevier.

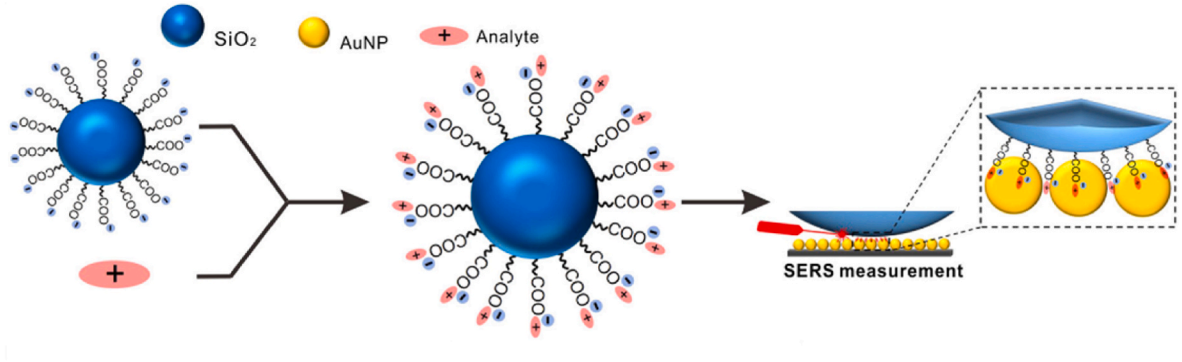

Fig. 9. (a) Schematic graph displaying the capture of the SERS measurement through the optoplasmonic structure. Reprinted with permission from Ref. [121]. Copyright (2020) American Chemical Society.

M-AMP and AMPs respectively within ~1 min of reaction time.

An electrochemical sensor developed using AuNPs/MWCNT-Nafion modified SPE could detect the M-AMP in a wide dynamic range of 0.02–0.1 μM (LOD value = 6 nM) using square wave stripping voltammetry, while a narrow detection range of 1.15–26.9 nM (LOD = 0.3 nM) could be achieved in the EIS mode [113]. Authors suggested that the uniform distribution of the AuNP over the MWCNTs-Nf/SPE and their synergistic effect towards the faster electron transfer could greatly improve the sensor performance to about 34 and 2.9 folds compared to the bare SPE and MWCNTs-Nf/SPE, respectively when measured using cyclic voltammetry (Fig. 8). Although the sensor exhibited a good detection range, the efficacy of the technique in real-life complex samples is yet to be established. In another example, a fast Fourier transform-square wave voltammetry (FFT-SWV) based hybrid electrochemical sensor was developed using a carbon paste electrode that was concurrently modified with MIP and MWCNTs [118]. This sensor displayed an excellent sensitivity with a LOD of 0.83 nM and two linear concentration ranges of 10 nM-1 μM and 3–100 μM. The sensor showed

Table 6
Overview of electrochemical and optical sensor technologies developed for the detection of benzodiazepines.

Illicit drug	Transducing mechanism	Sensor matrix	Sample matrix	LOD	Sensor characteristics	References
Flunitrazepam	DPV	CPE	KNO_3 Serum Urine	0.127 μM (KNO_3) 4.79 μM (serum/urine)	DR = 0.64–1.28 μM (KNO_3)	[132]
Flunitrazepam	DPV	$MnFe_2O_4$NPs/CPE	BRB Plasma	0.33 μM (BRB)	DR = 0.1–100 μM RP = 97–104%	[133]
Flunitrazepam	EIS	TiO_2@CuO–*N*-rGO/poly (L-Cys)/GCE	PBS Tourtel Malt Pepsi Cola Plasma	0.3 nM (PBS)	DR = 1 nM - 50 μM RP = 80–96.40% (tourtel malt) RP = 80–105.06% (pepsi cola) RP = 90–105.06% (Plasma)	[134]
Nitrazepam	DPV	AuNPs/rGO/GCE	PBS Serum Tablet	0.166 μM (PBS)	DR = 0.5–400 μM (PBS) RP = 99–102.4% (serum) RP = 99.3–101.6% (tablet)	[135]
Clonazepam	CV	SFs/IL/GCE	PBS Serum Urine	0.066 μM (PBS)	DR = 0.1–250 μM (PBS) RP = 97.2–103.2% (urine) RP = 101–99.1% (serum)	[129]
Clonazepam	CV	AgNPs/MWCNTs/GCE	PBS Serum Tablet	6 nM (PBS)	DR = 50 nM - 2.5 μM (PBS) RP = 96.5–107.5% (serum) RP = 95.5–106.5% (tablet)	[136]
Flunitrazepam	DPV	β-CD/B-RGO/GCE	PBS Serum	0.6 nM (PBS)	DR = 2.0 nM - 0.5 μM (PBS) RP = 89.0–109.0% (serum)	[130]
Diazepam	DPV	AgNDs/GNs/GC	PBS Plasma	85.6 nM (PBS)	DR = 100 nM - 20 μM (PBS) RP = 97.5–110% (plasma)	[137]
Diazepam	AdSV	SPCE	PBS with 10% ethanol	6.33 μM	DR = 25–1003 μM	[138]
Flunitrazepam	CV	SPGE	PBS Beverages	1.50 μM (PBS)	DR = 3.19–304 μM (PBS) DR = 3.19–76.67 μM (beverages)	[139]
Diazepam Flunitrazepam Lorazepam	CV	MNP-graphite epoxy sensor array	Britton-Robinson buffer	6.0 μM (diazepam) 5.6 μM (flunitrazepam) 4.6 μM (lorazepam)	DR = 35–110 μM (diazepam) DR = 32–960 μM (flunitrazepam) DR = 31–93 μM (lorazepam)	[131]
Lorazepam	EIS	Polypyrrole@sol-gel@AuNPs-MIP/PGE	PBS Tablet Urine Plasma	0.09 nM (PBS)	DR = 0.2–2.0 nM; DR = 2–20 nM (PBS) RP = 96–108% (tablet/urine/plasma)	[140]

Footnotes: AdSV = Adsorptive stripping voltammetry; AuNPs = Gold nanoparticles; AgNDs = Silver nanodendrimers; β-CD = β-cyclodextrin; B-RGO = Boron-doped reduced graphene oxide; CPE = Carbon paste electrode; CV = Cyclic voltammetry; DPV = Differential pulse voltammetry; DR = Dynamic range; EIS = electrochemical impedance spectroscopy; GCE = Glassy carbon electrode; GNs/GCE = Graphene nanosheets modified glassy carbon electrode; LOD = Limit of detection; MIP = Molecularly imprinted polymer; $MnFe_2O_4$ = manganese (II) ferrite bimetallic oxides; MNP = Metal nanoparticle; MWCNT = Multi-walled carbon nanotubes; PBS = Phosphate buffer saline; PGE = pencil graphite electrode; rGO = reduced graphene oxide; RP = recovery percentage; SFs/IL = Silver fibers and ionic liquid nanocomposite; SPGE = Screen-printed graphite electrode.

94–104% recovery percentage with an RSD value of 1–3.5% when M-AMP was measured in the serum and urine samples. The high sensitivity of the system was attributed to the proficient charge transfer and increased active surface area due to the presence of CNTs that facilitated adsorption of a greater number of analyte molecules, while the presence of MIP dictated the high selectivity of the system for M-AMP detection.

Farahani et al. developed a fluorescent nanosensor by utilizing MIP-containing fluorescent graphene quantum dots (GQDs) for the detection of M-AMP [119]. The M-AMP molecules interact with the carboxyl groups present at the surface of GQDs@MIP through hydrogen bonding causing an energy transfer from the excited GQDs@MIP to M-AMP, which eventually quenches the fluorescence intensity of the GQD. The sensor could achieve the detection limit of 1.7 μg/L for M-AMP even in the presence of AMP, codeine, morphine, and ibuprofen. On contrary, an enhancement in the fluorescence intensity was observed, when the nanosensor composed of carbon QDs (CQDs) and mesoporous structured imprinting microspheres interacted with M-AMP molecules [120]. This was attributed to the passivation and adjustment of active clusters present on the surface of CQDs. Under the optimized conditions, the fluorescent nanosensor displayed a linear dynamic range from 5.0 to 250 μM and a detection limit of 1.6 μM with a good recovery rate of 92–110% in urine and plasma samples. Due to adequate figures of merit of this sensor, it can be adapted for POC diagnostics for MA detection in biological settings.

The potential of SPR sensors based on indirect competitive immunoassay has also been investigated for the detection of M-AMP [116]. This system consists of a biosensing surface having immobilized M-AMP-BSA conjugate (M-AMP-BSA) which served as a competitor for antibody binding against M-AMP antigen in the sample. The method involved the filtration of the oral fluid sample followed by centrifugation and addition of antibody and then the introduction of the mixture to the sensor chip for analysis. The best performance was observed at a pH of 5.0 with good reusability of about 50 times with a coefficient of variation of 2.15%. The sensor could detect the M-AMP within 3 min with a LOD value of 0.44 ng/mL. The SPR based technique is quite simple, quick, sensitive, and repeatable, and has a good chance to develop into a POC device when integrated with a miniaturized SPR sensor platform [123]. In a recent study, Hong et al. developed an optoplasmonic hybrid material-based SERS sensor for ultrasensitive detection of M-AMP in the biological fluids (Fig. 9) [121]. The SERS substrate was fabricated by initially forming a self-assembled monolayer of AuNPs on a silicon chip followed by the deposition of analyte adsorbed SiO_2 microspheres (size = 5 μm). This hybrid material resulted in a strong Raman signal towards the sensitive quantification of M-AMP at 1001 and 1030 cm^{-1} peaks in saliva and urine samples. However, the assimilation of this sensing modality with futuristic technologies is essentially needed to develop a POC testing device.

2.5. Sensors for benzodiazepines

Benzodiazepines act by enhancing the γ-aminobutyric acid A ($GABA_A$) receptor function in the central nervous system which is highly addictive. These are therapeutically used for the treatment of insomnia, anxiety, depression, alcohol withdrawal symptoms, and also as a premedication for dental or surgical processes in the predetermined amount [124]. Overdose of BZDs causes sedation and muscle relaxing euphoria which has severe implications like hypotension, impulsive behavior, depersonalization, body coordination impairment, liver toxicity, which consequently lead to addiction and in turn lethal withdrawal symptoms [125,126]. Depending on the type of BZDs, it has a half-life ranging from 1 to 250 h; Higher the half-life, the more the complications, and the greater is the need for its detection for public safety and well-being [127]. The organization like DRUID has set their concentration limit up to 1–5 ng/mL in saliva for monitoring road safety. Several immunological detection kits like DrugWipe® 5+, rapid STAT® can meet this detection limit [128].

Recently, the usage of nanomaterials in both electrochemical and optical sensors has leveraged various innovative miniaturized systems for easy and rapid detection of BZDs (Table 6). For example, the catalytic properties of the silver nanofiber have been employed to develop an electrochemical sensor, where the GCE deposited with a nanocomposite of silver nanofibers/ionic liquid showed synergistic action for amplified sensor response [129]. The sensor exhibited the LOD value of 0.066 μM with a detection range of 0.1–250 μM with considerable reproducibility in the real urine and serum samples. Another modification of GCE with β-cyclodextrin/(β-CD)-boron-doped reduced graphene oxide (B-RGO) displayed a detection limit of 6 nM with a detection range of 0.002–0.5 μM for flunitrazepam, proving its potential for further development as a POC device [130]. Further advancement has been achieved recently in the form of the electronic tongue fabricated as an array-based voltammetric sensor for simultaneous detection of diazepam, flunitrazepam, and lorazepam with a unique combination of electrochemistry and machine learning [131]. In this approach, six different composite electrodes, i.e., CuO nanoparticles modified graphite electrode, Cu nanoparticles modified graphite electrode, Pt nanoparticles modified graphite electrode, WO_3 nanoparticles modified graphite electrode, pristine electrodes of epoxy-graphite, and Pt metal electrode have been utilized. To achieve proper discrimination among the BZDs and to predict their respective concentrations in the mixture, multivariate examination using principal component analysis (PCA) was carried out. This predictive model could be validated successfully by external test data set with an error as low as 0.5. Despite the reproducible, rapid, and sensitive detection, this system needs to be investigated and optimized on various other biological matrices [131].

Another comprehensive work by Yen et al. focused on the use of hydrophobic-carbon dots (hC-dots) for fluorescent detection of BZDs [141]. The hydrophobic nature of the hC-dots facilitated the binding to the hydrophobic BZDs which caused quenching of fluorescence

Table 7
Comparative analysis of conventional and point of care technology for illicit drug detection.

Illicit drug (sample matrix)	Recovery percentage POC technology	Recovery percentage conventional method (HPLC)	Advantages of POC over conventional method	References
Codeine (tablet)	98.5%	98%	Low-cost High stability Rapid analysis Good reproducibility	[90]
Methamphetamine (urine/ serum)	94.2% 92.8%	92.6% 90.3%	Simple in operation Cost-effective	[118]
Clonazepam (urine/serum)	97.2% 101.3%	101.2% 99.1%	Good reproducibility High stability	[129]
Diazepam (tablet)	98.84%	99.16%	Highly reliable No sample processing	[142]
Cocaine (urine)	96%	92.8%	One-step analysis Simplicity	[143]

intensity. Under optimized conditions, real-time analysis of nimetazepam could be displayed in the spiked sample (85 or 170 μM) prepared in beer, red wine, orange juice, and whiskey with the LOD of 7.24 μM.

3. Conclusion

Illicit drugs like COC, marijuana, OPs, AMPs, etc., despite their promising benefits as relaxants, anesthetics, pain killers, have become a serious concern for general health because of their increasing uncontrolled usage and occurrence in society. Biosensors are the fundamental tools that can help in the detection of administered illicit drugs having a restricted usage surpassing which may endanger the lives of several people due to their psychoactive effects. The aid of specialized biosensors for non-restricted drug use will also permit an understanding of the pharmacodynamic and pharmacokinetic effects of unlimited use of the drugs by the forensic laboratories and drug-supervising administration. The more versatile and label-free technique that allows for rapid on-site identification and quantification may help in various clinical aspects and applications. This review article depicted profiling of various optical and electrochemical sensors developed recently around the world for the detection of various illicit drugs. Such information provides a complete picture of the biosensor vulnerability and instability along with their promising effects. Depending upon the abundance of drugs or their metabolites in various sources, many commercial biosensors have demonstrated a narrow detection range to a certain drug(s) in the blood, saliva, urine, exhaled breath, and sweat.

Sensors listed in this review have shown many promising advantages like simplicity, real-time measurement, economic viability, low-cost for mass production, transport, storage, ease in the user interface implementation and disposal, no tedious sample preparation/complex pretreatment/requisition of trained personnel with the good precision in analysis (Table 7). Amongst the various sensing techniques, spectroscopy is the most convenient detection method as it provides easily distinguishable optical shift or intensity change without any additional requirement of a sophisticated instrument. Photoluminescence-based illicit drug sensing methods show greater potential with relatively very high sensitivity, however, the essential requirement of a sensitive photodetector, a specific light/laser source, and a set of specialized optical components can make the miniaturized device delicate and expensive. On the contrary, electrochemical sensors developed using gold, silver or carbon-based nanomaterials have demonstrated immense potential to realize into a field-deployable, hand-held POC device with ultra-high sensitivity and rapid detection. Further, these can be easily integrated with industry-ready technologies that are currently being used for various other analyte testing. Particularly, the development of sensor matrices derived with illicit drug-specific MIP or aptamer have greater opportunities due to their high selectivity, stability, and greater binding affinity and to realize them for multiplexed sensing.

Despite significant progress in biosensor development for illicit drug testing, there are a few domains that require significant improvement. Moderate sensitivity or LOD and large variations in the sensor's response, particularly in real samples, along with the false-negative/positive sensor response remain a big challenge when integrating with innovative technology. Therefore, the development of miniaturized, scalable, robust technology without compromising the selectivity and sensitivity is the need of the hour. In addition, innovative microarray technology having the potential to detect multiple illicit drugs simultaneously in a single biological sample will be an ideal choice. Before the commercialization of the developed biosensors, batch-testing, and validation of these devices is also a challenging task that should be completed judiciously. Hybrid combinatorial technology that utilizes electrochemical sensors, novel nanomaterials, and optics together has been underutilized and more efforts may prospect in this area [144–149]. We presume that many of these challenges will be addressed along with innovative technological advancements in the near future, as many research groups in association with industry partners are continuously working with the sole focus on translational research on the detection of illicit drugs. Furthermore, the challenge to meet the demand of POC testing devices, particularly in resource-limited settings, can be addressed by employing the smartphone-integrated customized microoptoelectromechanical adapters. From laboratory-level assay development to innovative technology integration, a growing number of research efforts continue to be reported toward the realization of next-generation standalone sensing platforms for the POC devices for illicit drug testing. Over the next few years, a few breakthroughs are expected in the field of multiplexed illicit drug testing devices through cutting-edge technologies that will surely enable us to achieve the performance of conventional laboratory-based analysis methods but at a relatively low cost and in a shorter duration.

Declaration of competing interest

The authors declare the following financial interests/personal relationships which may be considered as potential competing interests: Himanshu Bhatia is the CEO of Ricovr Healthcare Inc. USA, a start-up with its interests in oral diagnostic technologies. Other authors do not have any competing interests.

References

[1] D.R. W, Drug Use and Health Consequences, United Nations publication, 2020. Sales No. E.20.XI.6). Booklet 2 11.
[2] G.S. Wang, M.-C. Le Lait, S.J. Deakyne, A.C. Bronstein, L. Bajaj, G. Roosevelt, Unintentional pediatric exposures to marijuana in Colorado, 2009-2015, JAMA Pediatrics 170 (9) (2016) e160971, https://doi.org/10.1001/jamapediatrics.2016.0971, e160971.
[3] NIDA, What Is the Scope of Marijuana Use in the United States?, 2020. https://www.drugabuse.gov/publications/research-reports/marijuana/what-scope-marijuana-use-in-united-states.
[4] F. Merz, United Nations office on drugs and crime: world drug report 2017, SIRIUS – Zeitschrift für Strategische Analysen 2 (1) (2017) 85–86, https://doi.org/10.1515/sirius-2018-0016, 2018.
[5] A. Roche, K. Pidd, V. Kostadinov, Alcohol- and drug-related absenteeism: a costly problem, Aust. N. Z. J. Publ. Health 40 (3) (2016) 236–238, https://doi.org/10.1111/1753-6405.12414.
[6] E.W. Boyer, R. Fletcher, R.J. Fay, D. Smelson, D. Ziedonis, R.W. Picard, Preliminary efforts directed toward the detection of craving of illicit substances: the iHeal project, J. Med. Toxicol. 8 (1) (2012) 5–9, https://doi.org/10.1007/s13181-011-0200-4.
[7] E.W. Boyer, D. Smelson, R. Fletcher, D. Ziedonis, R.W. Picard, Wireless technologies, ubiquitous computing and mobile health: application to drug abuse treatment and compliance with HIV therapies, J. Med. Toxicol. 6 (2) (2010) 212–216, https://doi.org/10.1007/s13181-010-0080-z.
[8] R.R. Fletcher, S. Tam, O. Omojola, R. Redemske, J. Kwan, Wearable sensor platform and mobile application for use in cognitive behavioral therapy for drug addiction and PTSD, 2011, Annu. Int. Conf. IEEE Eng. Med. Biol. Soc. (2011) 1802–1805, https://doi.org/10.1109/iembs.2011.6090513.
[9] T. Joye, J. Sidibé, J. Déglon, A. Karmime, F. Sporkert, C. Widmer, B. Favrat, P. Lescuyer, M. Augsburger, A. Thomas, Liquid chromatography-high resolution mass spectrometry for broad-spectrum drug screening of dried blood spot as microsampling procedure, Anal. Chim. Acta 1063 (2019) 110–116, https://doi.org/10.1016/j.aca.2019.02.011.
[10] S.L. Kacinko, A.J. Barnes, I. Kim, E.T. Moolchan, L. Wilson, G.A. Cooper, C. Reid, D. Baldwin, C.W. Hand, M.A. Huestis, Performance characteristics of the Cozart® RapiScan oral fluid drug testing system for opiates in comparison to ELISA and GC/MS following controlled codeine administration, Forensic Sci. Int. 141 (1) (2004) 41–48, https://doi.org/10.1016/j.forsciint.2003.12.003.
[11] S. Wang, Y. Wei, H. Jin, C. Li, H. Du, A 96-well plate based dot-ELISA array for simultaneous detection of multi-drugs, Anal. Lett. 42 (17) (2009) 2807–2819, https://doi.org/10.1080/00032710903202030.
[12] United States Department of Health and Human Services Substance Abuse and Mental Health Services Administration Mandatory Guidelines for Federal Workplace Drug Testing Programs, Federal Register, 2008, pp. 71858–71907.
[13] E.P. Baron, Comprehensive review of medicinal marijuana, cannabinoids, and therapeutic implications in medicine and headache: what a long strange trip it's been, Headache 55 (6) (2015) 885–916, https://doi.org/10.1111/head.12570.
[14] E. Childs, J.A. Lutz, H. de Wit, Dose-related effects of delta-9-THC on emotional responses to acute psychosocial stress, Drug Alcohol Depend. 177 (2017) 136–144, https://doi.org/10.1016/j.drugalcdep.2017.03.030.
[15] M.P. Viveros, E.M. Marco, S.E. File, Endocannabinoid system and stress and anxiety responses, Pharmacol, Biochem. Behav. 81 (2) (2005) 331–342, https://doi.org/10.1016/j.pbb.2005.01.029.
[16] T. Blencowe, A. Pehrsson, P. Lillsunde, K. Vimpari, S. Houwing, B. Smink, R. Mathijssen, T. Van der Linden, S.-A. Legrand, K. Pil, A. Verstraete, An analytical evaluation of eight on-site oral fluid drug screening devices using

laboratory confirmation results from oral fluid, Forensic Sci. Int. 208 (1) (2011) 173–179, https://doi.org/10.1016/j.forsciint.2010.11.026.
[17] M.J. Swortwood, M.N. Newmeyer, O.A. Abulseoud, M. Andersson, A.J. Barnes, K. B. Scheidweiler, M.A. Huestis, On-site oral fluid Δ 9 -tetrahydrocannabinol (THC) screening after controlled smoked, vaporized, and oral cannabis administration, Forensic Toxicol. 35 (1) (2017) 133–145, https://doi.org/10.1007/s11419-016-0348-3.
[18] M. Sajid, A.-N. Kawde, M. Daud, Designs, formats and applications of lateral flow assay: a literature review, J. Saudi Chem. Soc. 19 (6) (2015) 689–705, https://doi.org/10.1016/j.jscs.2014.09.001.
[19] F. Musshoff, E.G.e. Hokamp, U. Bott, B. Madea, Performance evaluation of on-site oral fluid drug screening devices in normal police procedure in Germany, Forensic Sci. Int. 238 (2014) 120–124, https://doi.org/10.1016/j.forsciint.2014.02.005.
[20] S.C.D. Dobri, A.H. Moslehi, T.C. Davies, Are oral fluid testing devices effective for the roadside detection of recent cannabis use? A systematic review, Publ. Health 171 (2019) 57–65, https://doi.org/10.1016/j.puhe.2019.03.006.
[21] K. Dolan, D. Rouen, J. Kimber, An overview of the use of urine, hair, sweat and saliva to detect drug use, Drug Alcohol Rev. 23 (2) (2004) 213–217, https://doi.org/10.1080/09595230410001704208.
[22] M.J. Swortwood, M.N. Newmeyer, M. Andersson, O.A. Abulseoud, K. B. Scheidweiler, M.A. Huestis, Cannabinoid disposition in oral fluid after controlled smoked, vaporized, and oral cannabis administration, Drug Test. Anal. 9 (6) (2017) 905–915, https://doi.org/10.1002/dta.2092.
[23] E. Romano, C. Moore, T. Kelley-Baker, P.A. Torres-Saavedra, The utility of delta 9-tetrahydrocannabinol (THC) measures obtained from oral fluid samples in traffic safety, Traffic Inj. Prev. 20 (7) (2019) 667–672, https://doi.org/10.1080/15389588.2019.1635690.
[24] C. Wanklyn, D. Burton, E. Enston, C.-A. Bartlett, S. Taylor, A. Raniczkowska, M. Black, L. Murphy, Disposable screen printed sensor for the electrochemical detection of delta-9-tetrahydrocannabinol in undiluted saliva, Chem. Cent. J. 10 (2016), 1.10.1186/s13065-016-0148-1.
[25] M. Klimuntowski, M.M. Alam, G. Singh, M.M.R. Howlader, Electrochemical sensing of cannabinoids in biofluids: a noninvasive tool for drug detection, ACS Sens. 5 (3) (2020) 620–636, https://doi.org/10.1021/acssensors.9b02390.
[26] S. Eissa, R.A. Almthen, M. Zourob, Disposable electrochemical immunosensor array for the multiplexed detection of the drug metabolites morphine, tetrahydrocannabinol and benzoylecgonine, Microchimica Acta 186 (8) (2019) 523, https://doi.org/10.1007/s00604-019-3646-8.
[27] Q. Zhang, D. Berg, S.M. Mugo, Molecularly imprinted carbon based electrodes for tetrahydrocannabinol sensing, Inorg. Chem. Commun. 107 (2019) 107459, https://doi.org/10.1016/j.inoche.2019.107459.
[28] D. Lu, F. Lu, G. Pang, A novel tetrahydrocannabinol electrochemical nano immunosensor based on horseradish peroxidase and double-layer gold nanoparticles, Molecules 21 (10) (2016), https://doi.org/10.3390/molecules21101377.
[29] M.A. Balbino, M.M. de Menezes, I.C. Eleotério, A.A. Saczk, L.L. Okumura, H. M. Tristão, M.F. de Oliveira, Voltammetric determination of Δ9-THC in glassy carbon electrode: an important contribution to forensic electroanalysis, Forensic Sci. Int. 221 (1–3) (2012) 29–32, https://doi.org/10.1016/j.forsciint.2012.03.020.
[30] R.K. Mishra, J.R. Sempionatto, Z. Li, C. Brown, N.M. Galdino, R. Shah, S. Liu, L. J. Hubble, K. Bagot, S. Tapert, J. Wang, Simultaneous detection of salivary Δ9-tetrahydrocannabinol and alcohol using a wearable electrochemical ring sensor, Talanta 211 (2020) 120757, https://doi.org/10.1016/j.talanta.2020.120757.
[31] H. Stevenson, A. Bacon, K.M. Joseph, W.R.W. Gwandaru, A. Bhide, D. Sankhala, V.N. Dhamu, S. Prasad, A rapid response electrochemical biosensor for detecting THC in saliva, Sci. Rep. 9 (1) (2019) 12701, https://doi.org/10.1038/s41598-019-49185-y.
[32] Y. Mohsen, N. Gharbi, A. Lenouvel, C. Guignard, Detection of Δ9-Tetrahydrocannabinol, methamphetamine and amphetamine in air at low ppb level using a field asymmetric ion mobility spectrometry microchip sensor, Procedia Eng. 87 (2014) 536–539, https://doi.org/10.1016/j.proeng.2014.11.542.
[33] S.I. Hwang, N.G. Franconi, M.A. Rothfuss, K.N. Bocan, L. Bian, D.L. White, S. C. Burkert, R.W. Euler, B.J. Sopher, M.L. Vinay, E. Sejdic, A. Star, Tetrahydrocannabinol detection using semiconductor-enriched single-walled carbon nanotube chemiresistors, ACS Sens. 4 (8) (2019) 2084–2093, https://doi.org/10.1021/acssensors.9b00762.
[34] B.D. Plouffe, S.K. Murthy, Fluorescence-based lateral flow assays for rapid oral fluid roadside detection of cannabis use, Electrophoresis 38 (3–4) (2017) 501–506, https://doi.org/10.1002/elps.201600075.
[35] K. Sivashanmugan, Y. Zhao, A.X. Wang, Tetrahydrocannabinol sensing in complex biofluid with portable Raman spectrometer using diatomaceous SERS substrates, Biosensors 9 (2019) 125.
[36] J.-R. Lee, J. Choi, T.O. Shultz, S.X. Wang, Small molecule detection in saliva facilitates portable tests of marijuana abuse, Anal. Chem. 88 (15) (2016) 7457–7461, https://doi.org/10.1021/acs.analchem.6b01688.
[37] G. Demirel, H. Usta, M. Yilmaz, M. Celik, H.A. Alidagi, F. Buyukserin, Surface-enhanced Raman spectroscopy (SERS): an adventure from plasmonic metals to organic semiconductors as SERS platforms, J. Mater. Chem. C 6 (20) (2018) 5314–5335, https://doi.org/10.1039/c8tc01168k.
[38] C. Zong, M. Xu, L.-J. Xu, T. Wei, X. Ma, X.-S. Zheng, R. Hu, B. Ren, Surface-enhanced Raman spectroscopy for bioanalysis: reliability and challenges, Chem. Rev. 118 (10) (2018) 4946–4980, https://doi.org/10.1021/acs.chemrev.7b00668.
[39] X. Kong, X. Chong, K. Squire, A.X. Wang, Microfluidic diatomite analytical devices for illicit drug sensing with ppb-Level sensitivity, Sensor. Actuator. B Chem. 259 (2018) 587–595, https://doi.org/10.1016/j.snb.2017.12.038.
[40] A. Wohlfarth, H. Mahler, V. Auwärter, Rapid isolation procedure for Δ9-tetrahydrocannabinolic acid A (THCA) from Cannabis sativa using two flash chromatography systems, J. Chromatogr. B 879 (28) (2011) 3059–3064, https://doi.org/10.1016/j.jchromb.2011.09.012.
[41] X. Kong, K. Squire, X. Chong, A.X. Wang, Ultra-sensitive lab-on-a-chip detection of Sudan I in food using plasmonics-enhanced diatomaceous thin film, Food Control 79 (2017) 258–265, https://doi.org/10.1016/j.foodcont.2017.04.007.
[42] E. Brunelle, B. Thibodeau, A. Shoemaker, J. Halámek, Step toward roadside sensing: noninvasive detection of a THC metabolite from the sweat content of fingerprints, ACS Sens. 4 (12) (2019) 3318–3324, https://doi.org/10.1021/acssensors.9b02020.
[43] H. Mirzaei, A. O'Brien, N. Tasnim, A. Ravishankara, H. Tahmooressi, M. Hoorfar, Topical review on monitoring tetrahydrocannabinol in breath, J. Breath Res. 14 (3) (2020), 034002, https://doi.org/10.1088/1752-7163/ab6229.
[44] P. Trefz, S. Kamysek, P. Fuchs, P. Sukul, J.K. Schubert, W. Miekisch, Drug detection in breath: non-invasive assessment of illicit or pharmaceutical drugs, J. Breath Res. (2017) 24001.
[45] T.M. Lovestead, T.J. Bruno, Determination of cannabinoid vapor pressures to aid in vapor phase detection of intoxication, Forensic Chem. 5 (2017) 79–85, https://doi.org/10.1016/j.forc.2017.06.003.
[46] P. Kintz, P. Mura, C. Jamey, J.-S. Raul, Detection of Δ9-tetrahydrocannabinol in exhaled breath after cannabis smoking and comparison with oral fluid, Forensic Toxicol. 35 (1) (2017) 173–178, https://doi.org/10.1007/s11419-016-0333-x.
[47] J.A. Hubbard, B.E. Smith, P.M. Sobolesky, S. Kim, M.A. Hoffman, J. Stone, M. A. Huestis, D.J. Grelotti, I. Grant, T.D. Marcotte, R.L. Fitzgerald, Validation of a liquid chromatography tandem mass spectrometry (LC-MS/MS) method to detect cannabinoids in whole blood and breath, Clin. Chem. Lab. Med. 58 (5) (2020) 673–681, https://doi.org/10.1515/cclm-2019-0600.
[48] N.L. Benowitz, Clinical pharmacology and toxicology of cocaine, Pharmacol. Toxicol. 72 (1) (1993) 3–12, https://doi.org/10.1111/j.1600-0773.1993.tb01331.x.
[49] W.W. Weddington, B.S. Brown, C.A. Haertzen, E.J. Cone, E.M. Dax, R.I. Herning, B.S. Michaelson, Changes in mood, craving, and sleep during short-term abstinence reported by male cocaine addicts: a controlled, residential study, Arch. Gen. Psychiatr. 47 (9) (1990) 861–868, https://doi.org/10.1001/archpsyc.1990.01810210069010.
[50] M. de Jong, A. Florea, A.-M.d. Vries, A.L.N. van Nuijs, A. Covaci, F. Van Durme, J. C. Martins, N. Samyn, K. De Wael, Levamisole: a common adulterant in cocaine street samples hindering electrochemical detection of cocaine, Anal. Chem. 90 (8) (2018) 5290–5297, https://doi.org/10.1021/acs.analchem.8b00204.
[51] M. de Jong, N. Sleegers, J. Kim, F. Van Durme, N. Samyn, J. Wang, K. De Wael, Electrochemical fingerprint of street samples for fast on-site screening of cocaine in seized drug powders, Chem. Sci. 7 (3) (2016) 2364–2370, https://doi.org/10.1039/c5sc04309c.
[52] J.M.P.J. Garrido, F. Borges, C.M.A. Brett, E.M.P.J. Garrido, Carbon nanotube β-cyclodextrin-modified electrode for quantification of cocaine in seized street samples, Ionics 22 (12) (2016) 2511–2518, https://doi.org/10.1007/s11581-016-1765-3.
[53] L. Asturias-Arribas, M.A. Alonso-Lomillo, O. Domínguez-Renedo, M.J. Arcos-Martínez, CYP450 biosensors based on screen-printed carbon electrodes for the determination of cocaine, Anal. Chim. Acta 685 (1) (2011) 15–20, https://doi.org/10.1016/j.aca.2010.11.006.
[54] J.C. Vidal, J.R. Bertolín, L. Bonel, L. Asturias, M.J. Arcos-Martínez, J.R. Castillo, A multi-electrochemical competitive immunosensor for sensitive cocaine determination in biological samples, Electroanalysis 28 (4) (2016) 685–694, https://doi.org/10.1002/elan.201500517.
[55] F. Shahdost-fard, M. Roushani, Conformation switching of an aptamer based on cocaine enhancement on a surface of modified GCE, Talanta 154 (2016) 7–14, https://doi.org/10.1016/j.talanta.2016.03.055.
[56] B. Jiang, M. Wang, Y. Chen, J. Xie, Y. Xiang, Highly sensitive electrochemical detection of cocaine on graphene/AuNP modified electrode via catalytic redox-recycling amplification, Biosens. Bioelectron. 32 (1) (2012) 305–308, https://doi.org/10.1016/j.bios.2011.12.010.
[57] M. Roushani, F. Shahdost-fard, Fabrication of an electrochemical nanoaptasensor based on AuNPs for ultrasensitive determination of cocaine in serum sample, Mater. Sci. Eng. C 61 (2016) 599–607, https://doi.org/10.1016/j.msec.2016.01.002.
[58] L. Asturias-Arribas, M.A. Alonso-Lomillo, O. Domínguez-Renedo, M.J. Arcos-Martínez, Electrochemical determination of cocaine using screen-printed cytochrome P450 2B4 based biosensors, Talanta 105 (2013) 131–134, https://doi.org/10.1016/j.talanta.2012.11.078.
[59] N.A. Abdelshafi, J. Bell, K. Rurack, R.J. Schneider, Microfluidic electrochemical immunosensor for the trace analysis of cocaine in water and body fluids, Drug Test. Anal. 11 (3) (2019) 492–500, https://doi.org/10.1002/dta.2515.
[60] R. D'Aurelio, I. Chianella, J.A. Goode, I.E. Tothill, Molecularly imprinted nanoparticles based sensor for cocaine detection, Biosensors 10 (3) (2020) 22, https://doi.org/10.3390/bios10030022.
[61] Y. Li, X. Ji, B. Liu, Chemiluminescence aptasensor for cocaine based on double-functionalized gold nanoprobes and functionalized magnetic microbeads, Anal. Bioanal. Chem. 401 (1) (2011) 213–219, https://doi.org/10.1007/s00216-011-5064-6.
[62] M.P. Chantada-Vázquez, C. de-Becerra-Sánchez, A. Fernández-Del-Río, J. Sánchez-González, A.M. Bermejo, P. Bermejo-Barrera, A. Moreda-Piñeiro,

Development and application of molecularly imprinted polymer - Mn-doped ZnS quantum dot fluorescent optosensing for cocaine screening in oral fluid and serum, Talanta 181 (2018) 232–238, https://doi.org/10.1016/j.talanta.2018.01.017.
[63] L. Qiu, H. Zhou, W. Zhu, L. Qiu, J. Jiang, G. Shen, R. Yu, A novel label-free fluorescence aptamer-based sensor method for cocaine detection based on isothermal circular strand-displacement amplification and graphene oxide absorption, New J. Chem. 37 (12) (2013) 3998–4003, https://doi.org/10.1039/C3NJ00594A.
[64] O. Adegoke, C. McKenzie, N.N. Daeid, Multi-shaped cationic gold nanoparticle-l-cysteine-ZnSeS quantum dots hybrid nanozyme as an intrinsic peroxidase mimic for the rapid colorimetric detection of cocaine, Sensor. Actuator. B Chem. 287 (2019) 416–427, https://doi.org/10.1016/j.snb.2019.02.074.
[65] Y. Qiu, Y. Tang, B. Li, M. He, Rapid detection of cocaine using aptamer-based biosensor on an evanescent wave fibre platform, R. Soc. Open Sci. 5 (10) (2018) 180821, https://doi.org/10.1098/rsos.180821.
[66] C.G. Bauer, A.V. Eremenko, A. Kühn, K. Kürzinger, A. Makower, F.W. Scheller, Automated amplified flow immunoassay for cocaine, Anal. Chem. 70 (21) (1998) 4624–4630, https://doi.org/10.1021/ac971388s.
[67] S. Song, L. Wang, J. Li, C. Fan, J. Zhao, Aptamer-based biosensors, TrAC Trends Anal. Chem. (Reference Ed.) 27 (2) (2008) 108–117, https://doi.org/10.1016/j.trac.2007.12.004.
[68] A.B. Iliuk, L. Hu, W.A. Tao, Aptamer in bioanalytical applications, Anal. Chem. 83 (12) (2011) 4440–4452, https://doi.org/10.1021/ac201057w.
[69] M. Roushani, F. Shahdost-fard, An aptasensor for voltammetric and impedimetric determination of cocaine based on a glassy carbon electrode modified with platinum nanoparticles and using rutin as a redox probe, Microchim. Acta 183 (1) (2016) 185–193, https://doi.org/10.1007/s00604-015-1604-7.
[70] M. Roushani, F. Shahdost-fard, A highly selective and sensitive cocaine aptasensor based on covalent attachment of the aptamer-functionalized AuNPs onto nanocomposite as the support platform, Anal. Chim. Acta 853 (2015) 214–221, https://doi.org/10.1016/j.aca.2014.09.031.
[71] R. Kawano, T. Osaki, H. Sasaki, M. Takinoue, S. Yoshizawa, S. Takeuchi, Rapid detection of a cocaine-binding aptamer using biological nanopores on a chip, JACS 133 (22) (2011) 8474–8477, https://doi.org/10.1021/ja2026085.
[72] J. Wang, J. Hou, H. Zhang, Y. Tian, L. Jiang, Single nanochannel-aptamer-based biosensor for ultrasensitive and selective cocaine detection, ACS Appl. Mater. Interfaces 10 (2) (2018) 2033–2039, https://doi.org/10.1021/acsami.7b16539.
[73] J. Chen, J. Jiang, X. Gao, G. Liu, G. Shen, R. Yu, A new aptameric biosensor for cocaine based on surface-enhanced Raman scattering spectroscopy, Chem. Eur J. 14 (27) (2008) 8374–8382, https://doi.org/10.1002/chem.200701307.
[74] J. Zhang, L. Wang, D. Pan, S. Song, F.Y.C. Boey, H. Zhang, C. Fan, Visual cocaine detection with gold nanoparticles and rationally engineered aptamer structures, Small 4 (8) (2008) 1196–1200, https://doi.org/10.1002/smll.200800057.
[75] K. Li, W. Qin, F. Li, X. Zhao, B. Jiang, K. Wang, S. Deng, C. Fan, D. Li, Nanoplasmonic imaging of latent fingerprints and identification of cocaine, Angew. Chem. Int. Ed. 52 (44) (2013) 11542–11545, https://doi.org/10.1002/anie.201305980.
[76] A.N. Nafziger, R.L. Barkin, Opioid therapy in acute and chronic pain, J. Clin. Pharmacol. 58 (9) (2018) 1111–1122, https://doi.org/10.1002/jcph.1276.
[77] M. Filizola, L.A. Devi, How opioid drugs bind to receptors, Nature 485 (7398) (2012) 314–317, https://doi.org/10.1038/485314a.
[78] P.A. Glare, T.D. Walsh, Clinical pharmacokinetics of morphine, Ther. Drug Monit. 13 (1) (1991) 1–23.
[79] C.M. Selavka, Poppy seed ingestion as a contributing factor to opiate-positive urinalysis results: the pacific perspective, J. Forensic Sci. 36 (3) (1991) 685–696, https://doi.org/10.1520/jfs13077j.
[80] P. Abraham, S. R, P. Vijayan, V. N, K. Sreevalsan, V. Anithakumary, Review on the progress in electrochemical detection of morphine based on different modified electrodes, J. Electrochem. Soc. 167 (3) (2020), 037559, https://doi.org/10.1149/1945-7111/ab6cf6.
[81] K. Eckart, J. Röhrich, D. Breitmeier, M. Ferner, R. Laufenberg-Feldmann, R. Urban, Development of a new multi-analyte assay for the simultaneous detection of opioids in serum and other body fluids using liquid chromatography–tandem mass spectrometry, J. Chromatogr. B 1001 (2015) 1–8, https://doi.org/10.1016/j.jchromb.2015.06.028.
[82] H. Ahmar, H. Tabani, M. Hossein Koruni, S.S.H. Davarani, A.R. Fakhari, A new platform for sensing urinary morphine based on carrier assisted electromembrane extraction followed by adsorptive stripping voltammetric detection on screen-printed electrode, Biosens. Bioelectron. 54 (2014) 189–194, https://doi.org/10.1016/j.bios.2013.10.035.
[83] A. Navaee, A. Salimi, H. Teymourian, Graphene nanosheets modified glassy carbon electrode for simultaneous detection of heroine, morphine and noscapine, Biosens. Bioelectron. 31 (1) (2012) 205–211, https://doi.org/10.1016/j.bios.2011.10.018.
[84] R.P. Talemi, M.H. Mashhadizadeh, A novel morphine electrochemical biosensor based on intercalative and electrostatic interaction of morphine with double strand DNA immobilized onto a modified Au electrode, Talanta 131 (2015) 460–466, https://doi.org/10.1016/j.talanta.2014.08.009.
[85] M. Tao, F. Xu, Y. Li, Q. Xu, Y. Chang, Y. Yang, Z. Wu, Amperometric morphine detection using pt-co alloy nanowire array-modified electrode, Bull. Kor. Chem. Soc. 31 (7) (2010) 1968–1972.
[86] B. Rezaei, S. Foroughi-Dehnavi, A.A. Ensafi, Fabrication of electrochemical sensor based on molecularly imprinted polymer and nanoparticles for determination trace amounts of morphine, Ionics 21 (10) (2015) 2969–2980, https://doi.org/10.1007/s11581-015-1458-3.
[87] M. Jahanbakhshi, In situ synthesis of rhodium nanoparticles mesoporous carbon hybrid via a novel and facile nanocasting method for simultaneous determination of morphine and buprenorphine, Mater. Sci. Eng. C 97 (2019) 479–485, https://doi.org/10.1016/j.msec.2018.12.019.
[88] N. Mohseni, M. Bahram, Mean centering of ratio spectra for colorimetric determination of morphine and codeine in pharmaceuticals and biological samples using melamine modified gold nanoparticles, Anal. Method. 8 (37) (2016) 6739–6747, https://doi.org/10.1039/c6ay02091g.
[89] J. Cao, X.-Y. Chen, W.-R. Zhao, Determination of morphine in human urine by the novel competitive fluorescence immunoassay, J. Anal. Method. Chem. 2019 (2019) 7826090, https://doi.org/10.1155/2019/7826090.
[90] A. Afkhami, H. Khoshsafar, H. Bagheri, T. Madrakian, Facile simultaneous electrochemical determination of codeine and acetaminophen in pharmaceutical samples and biological fluids by graphene–$CoFe_2O_4$ nanocomposite modified carbon paste electrode, Sensor. Actuator. B Chem. 203 (2014) 909–918, https://doi.org/10.1016/j.snb.2014.07.031.
[91] A. Afkhami, F. Gomar, T. Madrakian, $CoFe_2O_4$ nanoparticles modified carbon paste electrode for simultaneous detection of oxycodone and codeine in human plasma and urine, Sensor. Actuator. B Chem. 233 (2016) 263–271, https://doi.org/10.1016/j.snb.2016.04.067.
[92] A. Azadbakht, A.R. Abbasi, Engineering an aptamer-based recognition sensor for electrochemical opium alkaloid biosensing, J. Mater. Sci. Mater. Electron. 30 (4) (2019) 3432–3442, https://doi.org/10.1007/s10854-018-00618-w.
[93] L. Zeng, X.-P. Liu, H. Zhou, Z.-C. Liu, H.-X. Hao, Novel molecular imprinted polymer used to detect trace codeine on surface plasmon resonance, J. Pharmaceut. Med. (2016) 1020–1033.
[94] S.A. Goodchild, L.J. Hubble, R.K. Mishra, Z. Li, K.Y. Goud, A. Barfidokht, R. Shah, K.S. Bagot, A.J.S. McIntosh, J. Wang, Ionic liquid-modified disposable electrochemical sensor strip for analysis of fentanyl, Anal. Chem. 91 (5) (2019) 3747–3753, https://doi.org/10.1021/acs.analchem.9b00176.
[95] N. Wester, E. Mynttinen, J. Etula, T. Lilius, E. Kalso, B.F. Mikladal, Q. Zhang, H. Jiang, S. Sainio, D. Nordlund, E.I. Kauppinen, T. Laurila, J. Koskinen, Single-walled carbon nanotube network electrodes for the detection of fentanyl citrate, ACS Appl. Nano Mater. 3 (2) (2020) 1203–1212, https://doi.org/10.1021/acsanm.9b01951.
[96] A. Barfidokht, R.K. Mishra, R. Seenivasan, S. Liu, L.J. Hubble, J. Wang, D.A. Hall, Wearable electrochemical glove-based sensor for rapid and on-site detection of fentanyl, Sensor. Actuator. B Chem. 296 (2019) 126422, https://doi.org/10.1016/j.snb.2019.04.053.
[97] E. Sohouli, A.H. Keihan, F. Shahdost-fard, E. Naghian, M.E. Plonska-Brzezinska, M. Rahimi-Nasrabadi, F. Ahmadi, A glassy carbon electrode modified with carbon nanoonions for electrochemical determination of fentanyl, Mater. Sci. Eng. C 110 (2020) 110684, https://doi.org/10.1016/j.msec.2020.110684.
[98] S. Eissa, M. Zourob, Competitive voltammetric morphine immunosensor using a gold nanoparticle decorated graphene electrode, Microchim. Acta 184 (7) (2017) 2281–2289, https://doi.org/10.1007/s00604-017-2261-9.
[99] G. Sakai, K. Ogata, T. Uda, N. Miura, N. Yamazoe, A surface plasmon resonance-based immunosensor for highly sensitive detection of morphine, Sensor. Actuator. B Chem. 49 (1) (1998) 5–12, https://doi.org/10.1016/S0925-4005(98)00107-5.
[100] M. Masteri-Farahani, N. Mollatayefeh, Chiral colloidal CdSe quantum dots functionalized with cysteine molecules: new optical nanosensor for selective detection and measurement of morphine, Colloids Surf. Physicochem. Eng. Aspects 569 (2019) 78–84, https://doi.org/10.1016/j.colsurfa.2019.02.037.
[101] M. Alhaddad, S.M. Sheta, Dual naked-eye and optical chemosensor for morphine detection in biological real samples based on Cr(III) metal–organic framework nanoparticles, ACS Omega 5 (43) (2020) 28296–28304, https://doi.org/10.1021/acsomega.0c04249.
[102] M.H. Mashhadizadeh, F. Rasouli, Design of a new carbon paste electrode modified with TiO_2 nanoparticles to use in an electrochemical study of codeine and simultaneous determination of codeine and acetaminophen in human plasma serum samples, Electroanalysis 26 (9) (2014) 2033–2042, https://doi.org/10.1002/elan.201400141.
[103] A. Lodha, A. Pandya, P.G. Sutariya, S.K. Menon, A smart and rapid colorimetric method for the detection of codeine sulphate, using unmodified gold nanoprobe, RSC Adv. 4 (92) (2014) 50443–50448, https://doi.org/10.1039/c4ra06269h.
[104] R.S. Vardanyan, V.J. Hruby, Fentanyl-related compounds and derivatives: current status and future prospects for pharmaceutical applications, Future Med. Chem. 6 (4) (2014) 385–412, https://doi.org/10.4155/fmc.13.215.
[105] P. Armenian, K.T. Vo, J. Barr-Walker, K.L. Lynch, Fentanyl, fentanyl analogs and novel synthetic opioids: a comprehensive review, Neuropharmacology 134 (2018) 121–132, https://doi.org/10.1016/j.neuropharm.2017.10.016.
[106] B.-T. Wang, J.M. Colby, A.H.B. Wu, K.L. Lynch, Cross-reactivity of acetylfentanyl and risperidone with a fentanyl immunoassay, J. Anal. Toxicol. 38 (9) (2014) 672–675, https://doi.org/10.1093/jat/bku103.
[107] J.S. Warrington, A. Walsh, E. Baker, D. Lozier, A. Belec, Keeping up with fentanyl: failure to do so is not an option, J. Appl. Lab. Med. 3 (1) (2018) 148–151, https://doi.org/10.1373/jalm.2017.025510.
[108] E.S. Calipari, M.J. Ferris, Amphetamine mechanisms and actions at the dopamine terminal revisited, J. Neurosci. 33 (21) (2013) 8923–8925, https://doi.org/10.1523/jneurosci.1033-13.2013.
[109] R. Savoca, K.M. Rentsch, A.R. Huber, Diagnostic efficiency of different amphetamine screening tests – the search for an optimal cutoff, Clin. Chem. Lab. Med. 42 (9) (2004) 1063–1065, https://doi.org/10.1515/CCLM.2004.213.
[110] N.A. Desrosiers, G. Milman, D.R. Mendu, D. Lee, A.J. Barnes, D.A. Gorelick, M. A. Huestis, Cannabinoids in oral fluid by on-site immunoassay and by GC-MS

using two different oral fluid collection devices, Anal. Bioanal. Chem. 406 (17) (2014) 4117–4128, https://doi.org/10.1007/s00216-014-7813-9.
[111] S. Strano-Rossi, E. Castrignanò, L. Anzillotti, G. Serpelloni, R. Mollica, F. Tagliaro, J.P. Pascali, D. di Stefano, R. Sgalla, M. Chiarotti, Evaluation of four oral fluid devices (DDS®, Drugtest 5000®, Drugwipe 5+® and RapidSTAT®) for on-site monitoring drugged driving in comparison with UHPLC–MS/MS analysis, Forensic Sci. Int. 221 (1) (2012) 70–76, https://doi.org/10.1016/j.forsciint.2012.04.003.
[112] O. Adegoke, S. Zolotovskaya, A. Abdolvand, N.N. Daeid, Biomimetic graphene oxide-cationic multi-shaped gold nanoparticle-hemin hybrid nanozyme: tuning enhanced catalytic activity for the rapid colorimetric apta-biosensing of amphetamine-type stimulants, Talanta 216 (2020) 120990, https://doi.org/10.1016/j.talanta.2020.120990.
[113] B. Rafiee, A.R. Fakhari, M. Ghaffarzadeh, Impedimetric and stripping voltammetric determination of methamphetamine at gold nanoparticles-multiwalled carbon nanotubes modified screen printed electrode, Sensor. Actuator. B Chem. 218 (2015) 271–279, https://doi.org/10.1016/j.snb.2015.03.077.
[114] L. Anvari, S.M. Ghoreishi, F. Faridbod, M.R. Ganjali, Electrochemical determination of methamphetamine in human plasma on a nanoceria nanoparticle decorated reduced graphene oxide (rGO) glassy carbon electrode (GCE), Anal. Lett. 54 (15) (2021) 2509–2522, https://doi.org/10.1080/00032719.2021.1875229.
[115] M. Haghighi, M. Shahlaei, M. Irandoust, A. Hassanpour, New and sensitive sensor for voltammetry determination of Methamphetamine in biological samples, J. Mater. Sci. Mater. Electron. 31 (14) (2020) 10989–11000, https://doi.org/10.1007/s10854-020-03647-6.
[116] J. Wang, W. Yao, F. Meng, P. Wang, Y. Wu, B. Wang, A surface plasmon resonance immunoassay for the rapid analysis of methamphetamine in forensic oral fluid, J. Clin. Lab. Anal. 33 (9) (2019), e22993, https://doi.org/10.1002/jcla.22993.
[117] T.-C. Chang, C.-Y. Chiang, M.-H. Lin, I.K. Chen, L.-K. Chau, D.-S. Hsu, S.-S. Shieh, C.-J. Kuo, S.-C. Wang, Y.-f. Chen, Fiber optic particle plasmon resonance immunosensor for rapid and sensitive detection of methamphetamine based on competitive inhibition, Microchem. J. 157 (2020) 105026, https://doi.org/10.1016/j.microc.2020.105026.
[118] M. Akhoundian, T. Alizadeh, M.R. Ganjali, P. Norouzi, Ultra-trace detection of methamphetamine in biological samples using FFT-square wave voltammetry and nano-sized imprinted polymer/MWCNTs -modified electrode, Talanta 200 (2019) 115–123, https://doi.org/10.1016/j.talanta.2019.02.027.
[119] M. Masteri-Farahani, S. Mashhadi-Ramezani, N. Mosleh, Molecularly imprinted polymer containing fluorescent graphene quantum dots as a new fluorescent nanosensor for detection of methamphetamine, Spectrochim. Acta Mol. Biomol. Spectrosc. 229 (2020) 118021, https://doi.org/10.1016/j.saa.2019.118021.
[120] S. Mandani, B. Rezaei, A.A. Ensafi, Sensitive imprinted optical sensor based on mesoporous structure and green nanoparticles for the detection of methamphetamine in plasma and urine, Spectrochim. Acta Mol. Biomol. Spectrosc. 231 (2020) 118077, https://doi.org/10.1016/j.saa.2020.118077.
[121] Y. Hong, X. Zhou, B. Xu, Y. Huang, W. He, S. Wang, C. Wang, G. Zhou, Y. Chen, T. Gong, Optoplasmonic hybrid materials for trace detection of methamphetamine in biological fluids through SERS, ACS Appl. Mater. Interfaces 12 (21) (2020) 24192–24200, https://doi.org/10.1021/acsami.0c00853.
[122] J. Mao, Y. Kang, D. Yu, J. Zhou, Surface-enhanced Raman spectroscopy integrated with aligner mediated cleavage strategy for ultrasensitive and selective detection of methamphetamine, Anal. Chim. Acta 1146 (2021) 124–130, https://doi.org/10.1016/j.aca.2020.12.028.
[123] S. Nootchanat, W. Jaikeandee, P. Yaiwong, C. Lertvachirapaiboon, K. Shinbo, K. Kato, S. Ekgasit, A. Baba, Fabrication of miniature surface plasmon resonance sensor chips by using confined sessile drop technique, ACS Appl. Mater. Interfaces 11 (12) (2019) 11954–11960, https://doi.org/10.1021/acsami.9b01617.
[124] H. Möhler, J.M. Fritschy, U. Rudolph, A new benzodiazepine pharmacology, J. Pharmacol. Exp. Therapeut. 300 (1) (2002) 2–8, https://doi.org/10.1124/jpet.300.1.2.
[125] S.C. Licata, J.K. Rowlett, Abuse and dependence liability of benzodiazepine-type drugs: GABAA receptor modulation and beyond, Pharmacol. Biochem. Behav. 90 (1) (2008) 74–89, https://doi.org/10.1016/j.pbb.2008.01.001.
[126] J.D. Jones, S. Mogali, S.D. Comer, Polydrug abuse: a review of opioid and benzodiazepine combination use, Drug Alcohol Depend. 125 (1) (2012) 8–18, https://doi.org/10.1016/j.drugalcdep.2012.07.004.
[127] C.E. Griffin 3rd, A.M. Kaye, F.R. Bueno, A.D. Kaye, Benzodiazepine pharmacology and central nervous system-mediated effects, Ochsner J. 13 (2) (2013) 214–223.
[128] A. Pehrsson, T. Blencowe, K. Vimpari, K. Langel, C. Engblom, P. Lillsunde, An evaluation of on-site oral fluid drug screening devices drugwipe® 5+ and rapid stat® using oral fluid for confirmation analysis, J. Anal. Toxicol. 35 (4) (2011) 211–218, https://doi.org/10.1093/anatox/35.4.211.
[129] A. Khoshroo, L. Hosseinzadeh, A. Sobhani-Nasab, M. Rahimi-Nasrabadi, F. Ahmadi, Silver nanofibers/ionic liquid nanocomposite based electrochemical sensor for detection of clonazepam via electrochemically amplified detection, Microchem. J. 145 (2019) 1185–1190, https://doi.org/10.1016/j.microc.2018.12.049.
[130] M.H. Ghanbari, Z. Norouzi, M.M. Ghanbari, Using a nanocomposite consist of Boron-doped reduced graphene oxide and electropolymerized β-cyclodextrin for Flunitrazepam electrochemical sensor, Microchem. J. 156 (2020) 104994, https://doi.org/10.1016/j.microc.2020.104994.
[131] A. Herrera-Chacón, F. Torabi, F. Faridbod, J.B. Ghasemi, A. González-Calabuig, M. del Valle, Voltammetric electronic tongue for the simultaneous determination of three benzodiazepines, Sensors 19 (2019) 5002.
[132] L. Hernández, P. Hernández, M.H. Blanco, E. Lorenzo, E. Alda, Determination of flunitrazepam by differential-pulse voltammetry using a bentonite-modified carbon paste electrode, Analyst 113 (11) (1988) 1719–1722, https://doi.org/10.1039/AN9881301719.
[133] B.M. Asiabar, M.A. Karimi, H. Tavallali, M. Rahimi-Nasrabadi, Application of $MnFe_2O_4$ and AuNPs modified CPE as a sensitive flunitrazepam electrochemical sensor, Microchem. J. 161 (2021) 105745, https://doi.org/10.1016/j.microc.2020.105745.
[134] E. Sohouli, M. Ghalkhani, M. Rostami, M. Rahimi-Nasrabadi, F. Ahmadi, A noble electrochemical sensor based on TiO_2@CuO-N-rGO and poly (L-cysteine) nanocomposite applicable for trace analysis of flunitrazepam, Mater. Sci. Eng. C 117 (2020) 111300, https://doi.org/10.1016/j.msec.2020.111300.
[135] L. Fritea, F. Bănică, T.O. Costea, L. Moldovan, C. Iovan, S. Cavalu, A gold nanoparticles - graphene based electrochemical sensor for sensitive determination of nitrazepam, J. Electroanal. Chem. 830–831 (2018) 63–71, https://doi.org/10.1016/j.jelechem.2018.10.015.
[136] B. Habibi, M. Jahanbakhshi, Silver nanoparticles/multi walled carbon nanotubes nanocomposite modified electrode: voltammetric determination of clonazepam, Electrochim. Acta 118 (2014) 10–17, https://doi.org/10.1016/j.electacta.2013.11.169.
[137] M.R. Majidi, S. Ghaderi, K. Asadpour-Zeynali, H. Dastangoo, Synthesis of dendritic silver nanostructures supported by graphene nanosheets and its application for highly sensitive detection of diazepam, Mater. Sci. Eng. C 57 (2015) 257–264, https://doi.org/10.1016/j.msec.2015.07.037.
[138] K.C. Honeychurch, A. Crew, H. Northall, S. Radbourne, O. Davies, S. Newman, J. P. Hart, The redox behaviour of diazepam (Valium®) using a disposable screen-printed sensor and its determination in drinks using a novel adsorptive stripping voltammetric assay, Talanta 116 (2013) 300–307, https://doi.org/10.1016/j.talanta.2013.05.017.
[139] J.P. Smith, J.P. Metters, D.K. Kampouris, C. Lledo-Fernandez, O.B. Sutcliffe, C. E. Banks, Forensic electrochemistry: the electroanalytical sensing of Rohypnol® (flunitrazepam) using screen-printed graphite electrodes without recourse for electrode or sample pre-treatment, Analyst 138 (20) (2013) 6185–6191, https://doi.org/10.1039/C3AN01352A.
[140] B. Rezaei, M.K. Boroujeni, A.A. Ensafi, A novel electrochemical nanocomposite imprinted sensor for the determination of lorazepam based on modified polypyrrole@sol-gel@gold nanoparticles/pencil graphite electrode, Electrochim. Acta 123 (2014) 332–339, https://doi.org/10.1016/j.electacta.2014.01.056. Complete.
[141] Y.-T. Yen, Y.-S. Lin, T.-H. Chen, S.-C. Chyueh, H.-T. Chang, A carbon-dot sensing probe for screening of date rape drugs: nitro-containing benzodiazepines, Sensor. Actuator. B Chem. 305 (2020) 127441, https://doi.org/10.1016/j.snb.2019.127441.
[142] N. Ghorbani, S. Hosseinzadeh, S. Pashaei, A. Hosseinzadeh, H.A. Hamidi, Preparation of unique potentiometric carbon paste sensor for determination of diazepam in pharmaceutical applications, Int. J. Electrochem. Sci. 9 (2014) 3772–3783.
[143] E. Guler, G. Bozokalfa, B. Demir, Z.P. Gumus, B. Guler, E. Aldemir, S. Timur, H. Coskunol, An aptamer folding-based sensory platform decorated with nanoparticles for simple cocaine testing, Drug Test. Anal. 9 (4) (2017) 578–587, https://doi.org/10.1002/dta.1992.
[144] M. Roushani, H. Hosseini, B. Pakzad, Z. Rahmati, Two-dimensional mesoporous copper hydroxide nanosheets shelled on hollow nitrogen-doped carbon nanoboxes as a high performance aptasensing platform, ACS Sustain. Chem. Eng. 9 (33) (2021) 11080–11090, https://doi.org/10.1021/acssuschemeng.1c02822.
[145] M. Roushani, H. Hosseini, Z. Hajinia, Z. Rahmati, Rationally designed of hollow nitrogen doped carbon nanotubes double shelled with hierarchical nickel hydroxide nanosheet as a high performance surface substrate for cortisol aptasensing, Electrochim. Acta 388 (2021) 138608, https://doi.org/10.1016/j.electacta.2021.138608.
[146] M. Roushani, M. Sarabaegi, H. Hosseini, Flexible NiP_2@hollow N-doped nanocapsules/carbon nanofiber as a freestanding electrode for glucose sensing, Compos. Commun. 25 (2021) 100686, https://doi.org/10.1016/j.coco.2021.100686.
[147] Z. Rahmati, M. Roushani, H. Hosseini, Three-dimensional $NiCo_2O_4$ nanowires encapsulated in nitrogen-doped carbon networks as a high-performance aptamer stabilizer for impedimetric ultrasensitive detection of hepatitis C virus core antigen, Surf. Interfaces 22 (2021) 100813, https://doi.org/10.1016/j.surfin.2020.100813.
[148] M. Divagar, R. Gayathri, R. Rasool, J.K. Shamlee, H. Bhatia, J. Satija, V.V.R. Sai, Plasmonic fiberoptic absorbance biosensor (P-FAB) for rapid detection of SARS-CoV-2 nucleocapsid protein, IEEE Sensor. J. 21 (20) (2021) 22758–22766, https://doi.org/10.1109/jsen.2021.3107736.
[149] K. Theyagarajan, S. Yadav, J. Satija, K. Thenmozhi, S. Senthilkumar, Gold nanoparticle-redox ionic liquid based nanoconjugated matrix as a novel multifunctional biosensing interface, ACS Biomater. Sci. Eng. 6 (11) (2020) 6076–6085, https://doi.org/10.1021/acsbiomaterials.0c00807.